

CRANFIELD UNIVERSITY

LIUPING QIAO

Integrated Deposition and Machining of Aluminium Alloy using
WAAM

SCHOOL OF APPLIED SCIENCES

MSc by Research Thesis

Academic Year: 2012 - 2013

Supervisor: Dr.Jörn Mehnen and Prof.Stewart Williams

November 2013

CRANFIELD UNIVERSITY

SCHOOL OF APPLIED SCIENCES

MSc by Research Thesis

Academic Year 2012 - 2013

LIUPING QIAO

Integrated Deposition and Machining of Aluminium Alloy using
WAAM

Supervisor: Dr. Jörn Mehnert and Prof. Stewart Williams

November 2013

This thesis is submitted in partial fulfilment of the requirements for
the degree of Master of Science

© Cranfield University 2013. All rights reserved. No part of this
publication may be reproduced without the written permission of the
copyright owner.

ABSTRACT

Conventional manufacturing processes often require a large amount of machining and cannot satisfy the continuously increasing requirements of a sustainable, low cost, and environmentally friendly modern industry. To solve these problems, Wire and Arc Additive Manufacturing (WAAM) process is used, which has a much higher deposition rate than most other metal additive manufacture processes.

Integrated deposition and machining is a novel AM technique which combines deposition and milling in one process; the milling step on the top surface does not only ensure the fixed height increment of each layer, but also increases the surface quality of the deposited multi-layered structure. In addition, the internal and external surface profile can be machined to remove any remaining surface roughness to attain the desired high quality surface of a near-net shape metal part.

In this project, the research aims at integrating WAAM technology with subtractive technology using basic wall shaped part structures in the analysis for finding the relationship between milling amount, surface waviness and part fatigue life. The project also applied the integrated deposition and machining (milling & drilling) idea to introduce a new way of deep hole drilling, especially for small-dimensional deep holes, which can be used to structures that would be impossible to attain by traditional hole drilling methods.

Keywords:

Wire and Arc Additive Manufacturing, Integrated Deposition and machining, Dry Machining, Near-net shape, Small-dimensional deep hole drilling

ACKNOWLEDGEMENTS

I would like to give my great gratitude to my supervisors Prof. Stewart Williams, Dr. Jialuo Ding and Dr. Jörn Mehnert for their guidance and help of my project.

My special gratitude is to Dr. Fude Wang and Mr. Braine Brooks for the technical assistance during the experimental work. In addition, I should thank Mr. Flemming Nielson for his help in practical work.

It is a pleasure to thank staffs and PhD students in Welding Engineering Research Centre for sharing their past findings and experience to my project.

Finally, I would also like to thank Mr. Andrew Dyer for his guidance in grinding experiment samples and taking images with microscope in the metallographic laboratory.

TABLE OF CONTENTS

ABSTRACT	i
ACKNOWLEDGEMENTS.....	iii
LIST OF FIGURES.....	vii
LIST OF TABLES	x
LIST OF EQUATIONS.....	xi
LIST OF ABBREVIATIONS	xii
1 Introduction.....	1
1.1 Research Background	1
1.2 Thesis Structure.....	2
1.3 Additional problems being considered	3
2 Literature Review	5
2.1 Additive Manufacturing	5
2.2 WAAM.....	6
2.3 Integrated deposition and machining	9
2.4 Surface geometry impact on fatigue cracking	11
2.5 From conventional wet machining to dry machining	13
2.6 Deep hole drilling	14
2.7 Research Gap.....	16
2.8 Summary	16
3 Aim and Objectives	19
3.1 Aim.....	19
3.2 Objectives	19
3.3 Project Scope	19
3.4 Methodology	19
3.4.1 Phase 1: Start of the research.....	20
3.4.2 Phase 2: Two experiments and analysis	20
3.4.3 Phase 3: Apply integrated deposition and machining process to deep hole drilling	21
3.4.4 Phase 4: Summary.....	22
4 Experiment on integrated deposition and machining.....	23
4.1 Introduction	23
4.2 Materials and experiment set-up.....	23
4.3 Fundamental characterization of single layer welds in aluminum alloy ...	25
4.3.1 Experimental condition for deposition.....	25
4.3.2 Results	26
4.3.3 Discussion.....	28
4.4 Experiment of multi-layer deposition in aluminum alloy	28
4.4.1 Parameters selection and methodology	28
4.4.2 Results	29
4.4.3 Discussion.....	30

4.5 Experiment of integrated deposition and machining in aluminum alloy...	31
4.5.1 Experiment	31
4.5.2 Results	33
4.5.3 Discussion.....	43
4.6 Experiment of integrated deposition and machining extended to mild steel	51
4.6.1 Experimental Setup for WAAM on mild steel.....	51
4.6.2 Measurement of the weld characteristics	53
4.6.3 Results	54
4.6.4 Discussion.....	57
4.7 Summary	58
5 Experiment on aluminum alloy of deep hole drilling	59
5.1 Introduction	59
5.2 Experiment.....	59
5.3 Results.....	62
5.3.1 Straightness of the hole.....	62
5.3.2 Depth of material coved on existing holes.....	63
5.4 Discussion	64
5.4.1 Advantages of this process for deep hole drilling	64
5.4.2 Research limitation.....	65
5.5 Summary	66
6 General Conclusions	67
7 Future Work.....	69
REFERENCES.....	71
APPENDICES	77
Appendix A Measurement of samples	77
Appendix B Obvious changes of notch in aluminium	80
Appendix C Problems that happened during the experiment.....	81

LIST OF FIGURES

Figure 1-1 Conventional machining method for wing ribs a) Aluminium billet, b) machined wing rib (CHIRON, 2012).....	1
Figure1-2 Thesis structure	3
Figure 2-1 CAD image of a teacup building using AM with different layer thicknesses (Gibson et al., 2010).....	5
Figure 2-2 Basic Additive Manufacture system (Ding, 2012).....	8
Figure 2-3 Products manufactured by WAAM	8
Figure 2-4 Process behaviour during CMT-PADV as a combination of CMT negative (-) and positive (+) current pulsing cycles (Fronius, 2010).....	9
Figure 2-5 Process principle of 3D Welding and Milling (Song et al., 2005).....	10
Figure 2-6 Face milling on weld deposition (Akula and Karunakaran, 2006)....	11
Figure 2-7 Circumferential notch (Rösler et al., 2007).....	12
Figure 2-8 Applications of deep hole drilling (Wei Hong co., Ltd).....	15
Figure 2-9 Deep hole drilling cycle by traditional drilling tools	15
Figure 3-1 Research methodology	20
Figure 3-2 Deep hole drilling strategy a) drilling process b) finished sample with some small-dimension holes.....	22
Figure 4-1 WAAM systems: a) HiVE machine b) Control console c) RCU 5000i control pendant	25
Figure 4-2 Measuring of macrograph single bead transverse with CMT-PADV process, W refers to bead width and H means bead height.....	27
Figure 4-3 Height and width of single beads at different wire feed speeds.....	28
Figure 4-4 Macroscopic cross section of single beads	28
Figure 4-5 a) WFS from 3.5 m/min to 7.5, b) method that substrate clamped on bed for 4 points, c) 10-layer welds with 9.0 m/min WFS and 0.6 m/min TS, d) 3-layer welds with 10.5 m/min WFS and 0.7 m/min TS.....	29
Figure 4-6 a) comparison of the two deposition walls with and without milling, b) cross section of the wall with milling.....	30
Figure 4-7 Process principle of integrated deposition and machining, a) WAAM process, b) Face milling process.....	31
Figure 4-8 Procedure of iterative deposition and face milling	32
Figure 4-9 Prescribed height for each layer of weld walls	32

Figure 4-10 Definition of milling amount for multi-layer walls	33
Figure 4-11 AMV 4000 machine.....	35
Figure 4-12 a) Method for measuring effective wall width, b) Method for measuring surface waviness	36
Figure 4-13 Cross-sectional macrographs of deposition welds with different milling amount.....	37
Figure 4-14 Polynomial trendline of scatter charts about relationship between milling amount and effective wall width at constant WFS/TS ration	37
Figure 4-15 Polynomial trendline of scatter charts about relationship between milling amount and surface waviness.....	38
Figure 4-16 Method for measuring the deposition efficiency	39
Figure 4-17 Polynomial trendline of scatter charts about relationship between milling amount and Material Efficiency	40
Figure 4-18 Measuring of the notch radius.....	41
Figure 4-19 Polynomial trendline of scatter chart about relationship between milling amount and notch radius.....	41
Figure 4-20 Stress concentration factor predictions from FEA model	42
Figure 4-21 Polynomial trendline of scatter charts about relationship between milling amount and stress concentration factor	43
Figure 4-22 the shape of last-layer weld bead of multi-layer with different WFS from 7.5 mm/min to 3.5 mm/min at constant WFS/TS ratio.....	44
Figure 4-23 Current and voltage in same welding parameters: a) Wave form of the CMT-PADV process for multi-layer welds in this project, b) Wave form of the CMT process for multi-layer welds (Cozzolino, 2013)	45
Figure 4-24 Sketch of samples with different overlap forms.....	46
Figure 4-25 Definition of macrograph cross section on multi-layer wall.....	46
Figure 4-26 Ideal model for overlap form	47
Figure 4-27 Geometry control by integrated deposition and machining process	48
Figure 4-28 Solubility of hydrogen in aluminium at various temperatures (Richard, 1995)	49
Figure 4-29 Scanning electron micrographs of longitude surface for sample with traditional WAAM process	50
Figure 4-30 Scanning electron micrographs of longitude surface for sample with integrated deposition and machining process	51

Figure 4-31 Experiment set-up for experiment on mild steel	53
Figure 4-32 Confocal laser scanning microscope.....	53
Figure 4-33 3D scanning view which records the contour curve between maximum data from peak and minimum data from valley in a setting region	54
Figure 4-34 Scatter chart about relationship between milling amount and Effective Wall Width (EWW).....	55
Figure 4-35 Scatter chart about relationship between milling amount and Surface Waviness (compare mild steel S235 with aluminium filler 4043) .	56
Figure 4-36 Scatter chart about relationship between milling amount and Material Efficiency (compare mild steel S235 with aluminium filler 4043) .	57
Figure 5-1 Experiment set-up for deep hole drilling.....	59
Figure 5-2 Procedure of drilling small-dimensional deep holes	60
Figure 5-3 Drill slips on the top of weld bead	61
Figure 5-4 Deep hole drilling strategy to see deposition effect on exist small holes	62
Figure 5-5 Structure manufactured by integrated deposition and machining (milling and drilling) process a) external front view of the structure b) photo of X-ray inspection c) top view of the structure.....	63
Figure 5-6 Depth measuring through X-ray inspection photo	64
Figure 5-7 X-ray inspection photo of sample without milling.....	65
Figure B- 1 The obvious changes of notch from sharp to flat with different milling amount increases from 25% to 70%	80
Figure C- 1 Walls got poor quality when there was no shielding gas during the deposition process	81
Figure C- 2 Too small WFS (first layer) resulted in low current and small dilution, layer seperated from substrate after milling was done.....	81
Figure C- 3 Joint flaws between wall and substrate, WFS set should be increased for the first layer	82
Figure C- 4 Holes present nearly folding line because of drill slipping the top of weld bead.....	82
Figure C- 5 Wrong setting of operating program resulted in the broken of workpiece and machining tool.....	83

LIST OF TABLES

Table 4-1: 4043 Alloy Classification Composition Requirement (Weight Percent)	23
Table 4-2: 2024 Alloy Classification Composition Requirement (Weight Percent)	24
Table 4-3: Experimental condition for deposition of 4043 Al-alloy.....	26
Table 4-4 Deposition conditions and bead characteristics of single layer welds	26
Table 4-5 Suitable milling parameter.....	33
Table 4-6 CMT-PADV for deposition parameters and calculation of heat input	35
Table 4-7 Measuring of the remelting area.....	47
Table 4-8 Chemical compositions of the mild steel substrates and solid wire electrodes (Weight Percent).....	51
Table 4-9 Deposition parameters of CMT for mild steel.....	52
Table 4-10 Experimental condition for depositing mild steel S235.....	52
Table A- 1 Detail data of samples with WFS at 7.5 m/min in al.....	77
Table A- 2 Detail data of samples with WFS at 6.5 m/min in al.....	77
Table A- 3 Detail data of samples with WFS at 5.5 m/min in al.....	78
Table A- 4 Detail data of samples with WFS at 4.5 m/min in al.....	78
Table A- 5 Detail data of samples with WFS at 3.5 m/min in al.....	79
Table A- 6 Detail data of samples with WFS at 7.0 m/min in mild steel.....	79

LIST OF EQUATIONS

Equation 4.1 Average welding arc power	34
Equation 4.2 Average welding arc energy	34
Equation 4.3 Calculation of heat input.....	34
Equation 5.1 Formula of calculating cutting speed (Brown and Sharpe, 2013)	61

LIST OF ABBREVIATIONS

AM	Additive Manufacturing
WAAM	Wire and Arc Additive Manufacturing
BTF	Buy-to-Fly
GTAW	Gas Tungsten Arc Welding
GMAW	Gas Metal Arc Welding
CMT	Cold Metal Transfer
CMT-PADV	CMT plus Pulse Advanced
MIG	Metal Inert Gas
MAG	Metal Active Gas
WFS	Wire Feed Speed
TS	Travel Speed
WD	Wire Diameter
SW	Surface Waviness
H	Bead Height
CA	Contact Angle
P	Penetration Depth
RA	Remelting Area
ME	Material Efficiency
SCF	Stress Concentration Factor
D	Dilution
HI	Heat Input
EWV	Effective Wall Width
FEA	Finite Element Analysis
SLS	Selective Laser Sintering
LENS	Laser Engineered Net Shaping
SLM	Selective Laser Melting
EBM	Electron Beam Melting
SL	Stereolithography
PWD	Plasma Wire Deposition
HLM	Hybrid-Layered Manufacturing
3D Welding	Three-dimensional Welding
RP	Rapid Prototyping
RS	Residual Stress
I	Welding current
DR	Deposition Rate
E	Young's modulus
CAD	Computer Aided Design

CTWD	Contact Tip to Work Distance
W	Bead Width
CLSM	Confocal Laser Scanning Microscopy
AE	Arc Energy
AIP	Average Instantaneous Power
CNC	Computer Numerical Control
I_{inst}	Instantaneous Current
LAM	Laser Additive Manufacturing
SDM	Shape Deposition Manufacturing
V_{inst}	Instantaneous Voltage
GMAW-P	Pulsed gas metal arc welding

1 Introduction

1.1 Research Background

Aluminium is the most widely used material in aerospace industry having continued to grow since the early 20th century. This material is used from 50% to 70% of the complete aircraft structures; the latest generation of airliners such as the A380 contains more than 60% by weight of aluminium alloy (Rendigs and Knowler, 2010) because of its excellent relation with regards for cost, density and strength, also easy manufacturability and metalwork capability.

When traditional machining processes are used, a vast amount of material is wasted; the Buy-to-Fly ration may be as high as 10 to 1 (Kazanas et al., 2012). The Buy-to-Fly ratio is defined as the ratio of mass of material that is required to machine a part to the mass of material in the finished part. It is obvious the smaller the value is, the more low-cost and efficient is the manufacturing process. Rib structures in aerospace for example (see Figure 1-1) are manufactured conventionally by milling away excess material from a billet of metal. This creates inevitable waste.

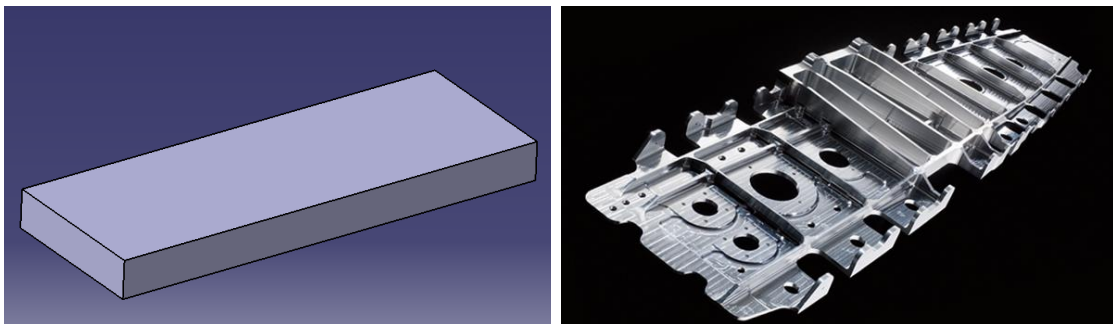


Figure 1-1 Conventional machining method for wing ribs a) Aluminium billet, b) machined wing rib (CHIRON, 2012)

Many industries are seeking for new fabrication processes, on the one hand for time saving, on the other hand for creating less waste. Wire and Arc Additive Manufacturing (WAAM) is a potential way forward to achieving this goal.

Integrated deposition and machining is one kind of Additive Manufacturing technique which combines deposition and milling in one process. The project

hypothesis that was that a milling step on the top of the added layer surface may not only ensure a fixed height increment of each layer, but also provides a flat surface for the subsequent layer thus helping to achieve near-net shape parts by mainly additive manufacturing only. Furthermore, milling on the top surface may also help in reducing the porosity problem which is due to defects in the top layer introduced by the welding process itself.

In this project, the research aims at combining WAAM technology and subtractive technologies for building wall structures for finding the relationship between milling amount, surface waviness and fatigue life. After certifying its fatigue performance in the acceptable scope, this process should be used to manufacture parts such as the ship propeller, deep slots and conformal cooling channel directly without end machining which are so complex geometrically structures with some special position impossible to be machined.

Finally, applying the integrated deposition and machining (milling & drilling) method on deep hole drilling, especially for small-dimensional deep holes, which can be used on structures that are impossible to attain by traditional hole drilling method.

1.2 Thesis Structure

Figure1-2 illustrates the thesis structure consisting of eight chapters. Chapter 1 introduces the research background, thesis structure, problem statement. In Chapter 2, a literature review related to this research topic is presented. Chapter 3 outlines the research aim, objectives and scope of this thesis. In addition, a detailed description of the methodology in each phase of this study is presented in this chapter. The main research outcomes of this project are elaborated in Chapter 4. It gives a description of materials and process, fundamental characterisation of single layer and multiple layers, facilities to be used in this research, method of measurement, deposition and milling parameters effect on weld bead shape, overlap style, surface waviness and fatigue life, a little section aims at seeing whether previous findings of relation between milling amount and surface waviness on aluminium can be generalised to other materials such as mild steel. Furthermore, results, analysis and

discussion are described in this chapter. In Chapter 5, a novel deep hole drilling technique is investigated, which applies previous findings and combining WAAM technology, dry milling and conventional dry drilling together to see the feasibility of fabricating deep hole drilling component. Chapter 6 gives an overall conclusion of the research project and Chapter 7 discusses the future work.

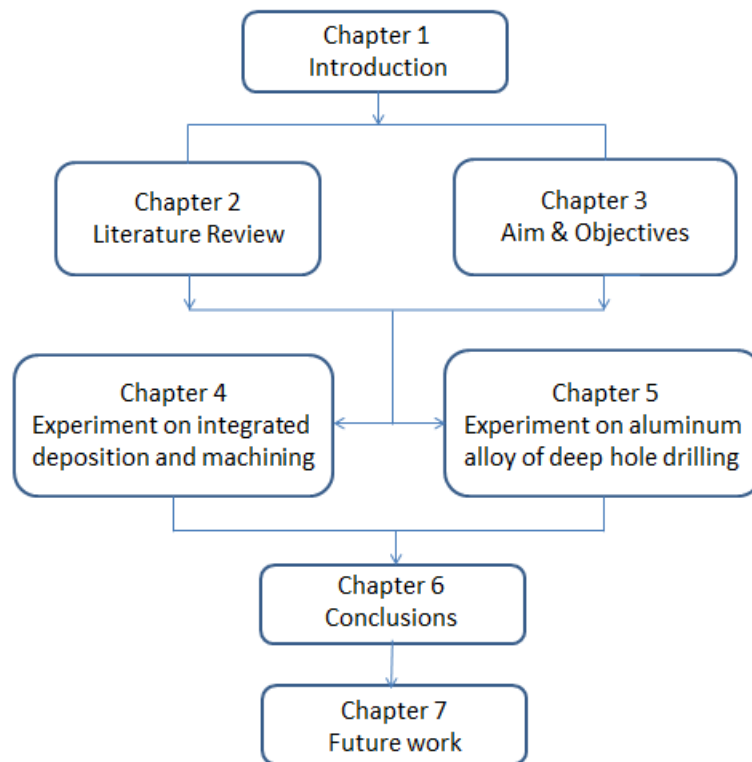


Figure1-2 Thesis structure

1.3 Additional problems being considered

The WAAM process has a much higher deposition rate and material usage efficiency than most other metal additive manufacture processes. Nevertheless, it can generate defects. Porosity is one of the major problems which always associated with the deposition of aluminium alloys. Fatigue test can only be done after the porosity problem has been solved.

The major machining method of this project is dry machining. When tools operate at high speed, a great thermal load is caused by friction between tool and workpiece. So one big challenges of dry machining is the problem of fast tool wear rates without cutting fluid. Another problem always accompanied by

dry machining is that chips may stick to the tool or part. Ribbon-like chips typically appeared at high machining temperatures which will affect the shape and dimensional accuracy of the machining surface. Thus, it was necessary to find a suitable tool with matching machining parameters that supports an integrated WAAM and machining process.

2 Literature Review

A comprehensive literature review has been carried out throughout the project duration. The literature includes the state-of-the-art research in Additive Manufacturing, Wire and Arc Additive Manufacturing, Integrated Deposition and machining, surface geometry impact on fatigue life, dry machining and deep hole drilling.

2.1 Additive Manufacturing

Additive Manufacturing (AM) is an innovative and very flexible technology that enables the making of complex net-shaped metal parts layer by layer. It has the advantage of reducing the amount of machining, as required by conventional approaches, hence reduces the negative waste of materials and having a lower influence on environment (Baufeld et al., 2010). As mentioned by Gibson et al., (2010), the AM technology which was used to be name as “Rapid Prototyping” was initially used for model making, then developed rapidly as materials, accuracy improved.



Figure 2-1 CAD image of a teacup building using AM with different layer thicknesses (Gibson et al., 2010)

Figure 2-1 shows a CAD image of a teacup built using AM with different layer thicknesses. The principle idea of this technology is to create a model through a three-dimensional Computer Aided Design (3D CAD) system and then fabricate the final geometry straight from the CAD file.

There are many kinds of additive manufacturing techniques such as plasma wire deposition, Electron Beam Melting, Selective Laser Sintering (SLS), stereolithography, 3D Welding, Laser Engineered Net Shaping (LENS), Wire

and Arc Additive Manufacturing (WAAM), etc. (Martina et al., 2012); (Zhai, 2012). Of course, these technologies have been applied to manufacture productions by several companies such as Siemens and Widex. At the same time, there are other hearing aid manufacturers use stereolithography (SL) to produce hearing aid shells, Align Technology used SL technology to produce clear braces. Boeing and its suppliers produced ducts and similar parts for F-18 fighter jets using selective laser sintering (SLS) (Rosen, 2007).

The combination of laser and powder is probably the most widely applied option. Santos et al., (2006) introduced various research efforts on Selective Laser Sintering (SLS), Selective Laser Melting (SLM) and 3-D Laser Cladding, which are the typical laser additive manufacturing systems to manufacture metal components. Components can be built with particular features and high accuracy when focusing laser power and feeding accurate controlled powder (Mok et al., 2008). However, it is also pointed that the dimension of the AM parts are constrained to a rather small scale because of the low deposition rate and complexity of the system. Song et al. (2005) mentioned the advantages of using lasers can produce high quality parts with good surface and accurate dimension, but the cost of investment is greatly higher compared to those fabricated with Gas Metal Arc Welding (GMAW).

Electron Beam Melting (EBM) is also a powder-based AM process, which was developed by Arcam AB, a Swedish technology development company (Kai et al., 2003). The power used in an EBM system is an electron beam in a high vacuum. Compared with a metal sintering process, the products of EBM demonstrate high quality, i.e. they are void-free, fully dense, and high strength properties. Taminger and Hafley (2002) found that Electron Beam Melting (EBM) of metals is in high energy efficient and is particularly suitable for handling with aluminium.

2.2 WAAM

Wire and Arc Additive Manufacturing (WAAM) is a manufacturing technique that can directly fabricate fully dense large 3-D near-net shape components from metal wire. In this process, wire is fed at a controlled rate into an electric arc

and is melted onto a substrate or the previously deposited layer (Wang et al., 2013). Martina et al., (2012) proved the feasibility of fabricating large aerospace structural components using Ti-6Al-4V with Plasma Deposition process, and found there were two advantages of this process such as higher effective wall width and deposition rate as compared to other AM processes. It also has higher material usage efficiency, no powder handling requirement, and a lower cost compared with the laser and powder-based technologies.

According to Ding et al., (2011), the WAAM process is a promising breakthrough of AM technology which combines electric arc heating sources with a metallic wire feeding system. The technique is a unique low cost solution for manufacturing large structural components in aerospace industry, and capital investment and “Buy-to-Fly” ratios can be significantly reduced because of short product development time with this process (Almeida and Williams, 2010). WAAM has the main advantages of high deposition rate, low cost of equipment installation and maintenance compared to laser-based powder and Electron Beam Melting processes (Chen, 2012).

Figure 2-2 shows the basic metal AM system which includes four portions: the main one is CNC controller and the other three are Material Supply system, Heat Source and Motion System (Ding, 2012). The WAAM system combines the standard wire based welding equipment and the common motion system such as industrial robots. Using the WAAM process can produce many detailed components which are required by industrial companies, see Figure 2-3.

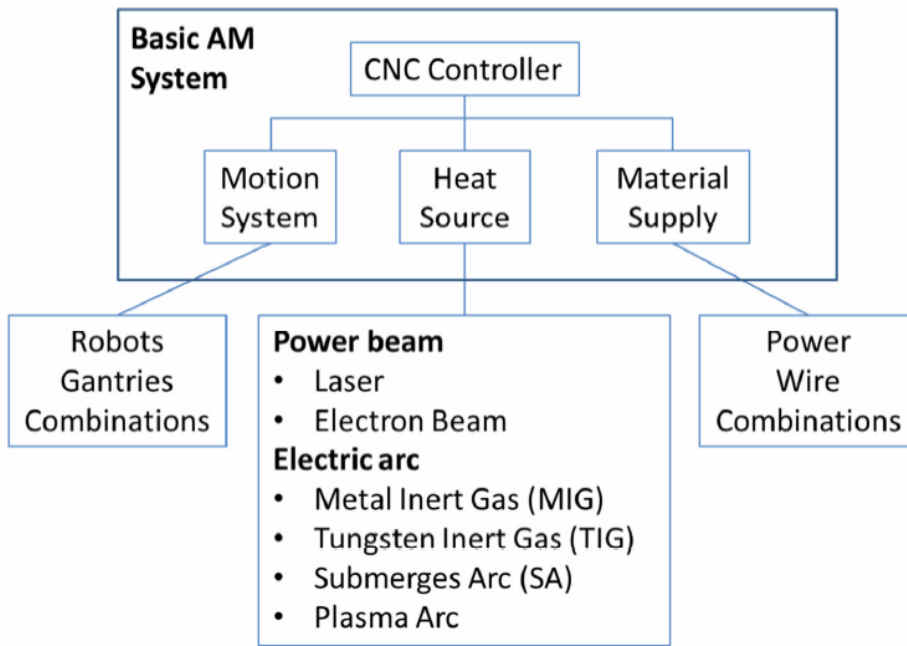


Figure 2-2 Basic Additive Manufacture system (Ding, 2012)



Figure 2-3 Products manufactured by WAAM

Gas Tungsten Arc Welding (GTAW) and Gas Metal Arc Welding (GMAW) are wire based welding techniques which can provide high deposition rates, however, they can also bring some problems like residual stress and distortion because of large heat input, these problems may have a detrimental impact on stability and accuracy of components and their mechanical properties (Mehnen et al., 2011). Fronius Cold Metal Transfer (CMT) is a particular type of GMAW process that was used for this study. It has the benefits of minimising the heat input into the weld/deposit, moreover, reducing defects such as porosity or hot cracking that could limit its development which is generated by welding. Legait (2006) added that the formation of gas porosity is one of the major issues associated with the welding of aluminium alloys. A new variant of this process, CMT plus Pulse Advanced (CMT-PADV) uses reverse polarity to reduce the heat input even further, it uses positive and negative polarity. When operating with negative polarity, there is more heating in the electrode than in the substrate, it reduces the overall heat input to the weld deposit and minimises dilution (Cozzolino, 2013). Figure 2-4 shows process behaviour during CMT-PADV by combining negatively poled CMT cycles and positively poled pulsing cycles.

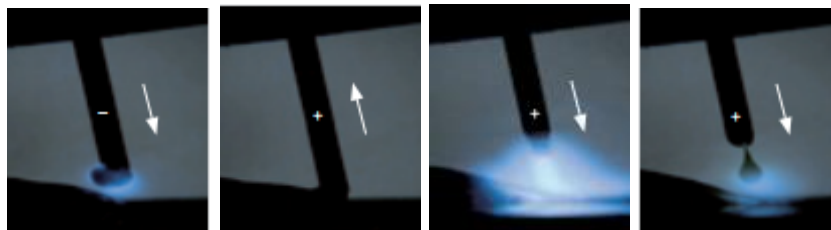


Figure 2-4 Process behaviour during CMT-PADV as a combination of CMT negative (-) and positive (+) current pulsing cycles (Fronius, 2010)

2.3 Integrated deposition and machining

The concept which integrates deposition and milling for one process was first presented by two research groups; the first group is from south Korea and another group is from the Indian Institute of Technology. The difference between them for directly prototyping of metallic parts is one combines welding

with 5-axis CNC milling and the other combines welding with 2.5-axis milling (Wang et al., 2004).

Song et al., (2005) created a new technology called “3D welding and milling” that combines welding as an additive process and milling as a subtractive process. This has many advantages compared to traditional way of manufacturing structures such as time saving for fabricating large scale structures and reducing tool wear for machining some high hardness materials. Thirdly, mixing techniques can be used to manufacture parts with some special position impossible to be machined, such as deep slots and conformal cooling channel.

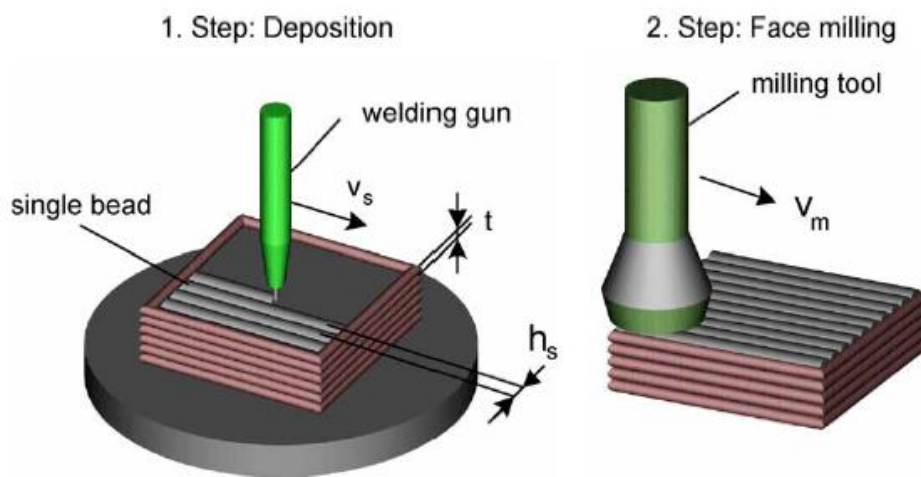


Figure 2-5 Process principle of 3D Welding and Milling (Song et al., 2005)

The process principle of 3D Welding and Milling is shown in Figure 2-5. When deposition is done, subsequent face milling is applied at the same setup to remove irregular material on the surface. By using this final surface finishing, any inaccurate dimension and geometry problems resulting from the deposition can be completely solved (Song et al., 2005).

Akula and Karunakaran (2006) investigated a new way of applying hybrid-layered manufacturing (HLM) process for rapid fabricating metallic moulds. This special approach combines MIG welding process and Computer Numerical Control (CNC) milling process, first for near-net shape and subsequent for net shape. They pointed out that step milling the top surface of the layer minimises

the deviation caused by welding process. It not only ensures the accuracy of vertical Z to attain the required layer thickness, but also removes the welded surface of possible oxidised layers which may influences the subsequent layer deposited on top of it. See Figure 2-6.

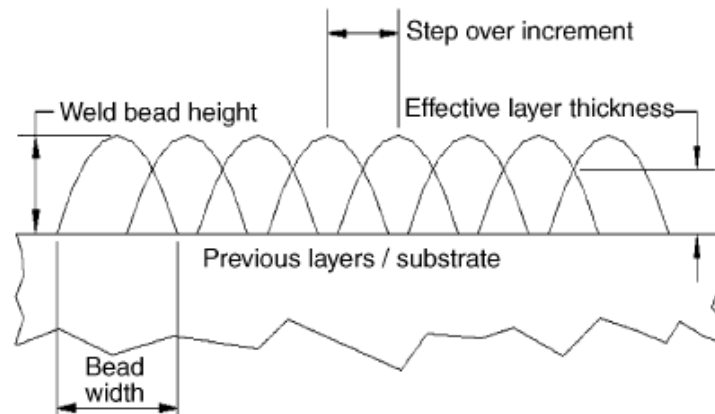


Figure 2-6 Face milling on weld deposition (Akula and Karunakaran, 2006)

These years, many researchers have paid attention on additional research work of hybrid processes. Taiwan University of Science and Technology used hybrid processes of selective laser cladding (SLC) and milling to fabricate metal rapid prototypes and molds (Jeng and Lin, 2001). In addition, Shape Deposition Manufacturing (SDM) of Stanford University (Fessler et al., 1996) and Controlled Metal Buildup (CMB) combined additive and subtractive techniques and make the deposition and the machining processes in the same setup. Similarly, the Research Centre for Advanced Manufacturing in the USA used a combination of abrasive water jet cutting, friction stir lap welding, and CNC machining to manufacture a complex-finned aluminium heat exchanger (SMU, 2012).

2.4 Surface geometry impact on fatigue cracking

It is widely known that residual stresses may give big influence on fatigue life of industrial components. Repeated wave loads in welds can cause fractures due to fatigue failure, which often occurs by initiation and subsequent growth of surface cracks in the weld toe region (Lassen, 1990). The term of weld stress concentration factor (SCF) is usually used to estimate fatigue crack initiation life

(Alam, 2012). As mentioned by Rösler et al., (2007), notches are sudden changes in the geometry of a component which can cause local stress concentrations and thus may induce premature failure, see Figure 2-7. The shape of notch radius in this project is similar to the circumferential notch which is between two layers.

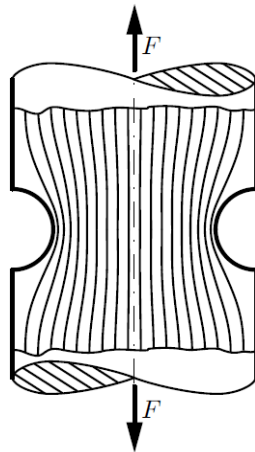


Figure 2-7 Circumferential notch (Rösler et al., 2007)

Webster and Ezeilo (2001) pointed out that tensile residual stress close to surface is prone to promote the initiation and spread of the fatigue process while compressive residual stresses near surface can give positive effect on fatigue life.

Sequeira Almeida (2012) has done some experiments on the single-layer and multi-layer deposition in steel, and observed the relationship between deposition parameter (including travel speed, wire feed speed and wire diameter), shielding gas and materials on surface waviness and effective wall width. Chapetti and Jaureguizar (2011) studied the effect of toe irregularity on fatigue resistance of welds and found that two factors, one is period of waves, another is local toe geometry, having strong impact on the fatigue crack initiation and propagation life. Long wave periods can give the longest fatigue life.

It is necessary to know how residual stresses generate and develop during WAAM in order to define potential strategies for mitigating their effects on distortion and mechanical properties (Sequeira Almeida, 2012)

2.5 From conventional wet machining to dry machining

Yue et al., (1999) found that more than 100 million gallons of metalworking fluids are used in the U.S. each year and that 1.2 million employees are exposed to them and to their potential health hazards.

As is widely known that cutting fluids have the function of cooling and lubricating to tools and workpieces during the whole machining operations, and thus improve tool life, make the surface smooth and accuracy-to-size, reduce process variability, friction reduction, cooling, corrosion protection, etc. (Adler et al., 2006). However, over the last two decade, it has been apparent that many metalworking fluids were sometimes unnecessary, cost of maintaining and disposing were high and cutting fluid mist may do harm to workers health (Canter, 2009). The manufacturing costs arrive at 16–20% when using coolants and lubricants for machining (Sreejith and Ngoi, 2000). Hence, all these have led to lower the application for metalworking fluids.

Sun et al., (2010) developed a new cooling method using cryogenic compressed air at high pressure (liquid nitrogen as coolant) to reduce the temperature of tool edge when cutting Ti–6Al–4V alloy. It was proved that chip temperature is lower by cryogenic compressed air cooling method compared to those by compressed air cooling and dry machining method. However, the spray of super cooled liquid nitrogen may also increase health hazards to the machine operator.

In view of the negative influence of cooling liquid on the environment and operator health, environmental friendly alternatives such as gaseous lubricants have been exploited. Junyan et al., (2010) investigated cutting operations with water vapour, gases (carbon dioxide, oxygen) or mixing water vapour & gas, finally found cutting force and cutting temperature were decreased a lot and tool life was extended much longer compared to dry cutting.

In fact, machining without the use of any coolant and lubricant has become a trend as a result of concerning the safety of the environment. An investigation has done by shown that suitable coatings have a great potential in the dry milling of Al alloys (Lahres et al., 1997). In addition, they also proved that

changing the machine technology, using appropriate cutting parameters and adapting the tool geometry can help reducing the temperature into a minimum with regard to dry machining.

Furthermore, choosing dry machining in this research is according to the necessity of integrated deposition and machining process. A study by Adebayo et al. (2013) has found that a mass of contamination in the deposited material when using solid lubricants, microstructure of the deposited material should be affected even though surface is cleaned by acetone prior to the weld deposition, To pursue dry machining, one way that has been studied is to take away the generated heat through indirect contact between coolants and workpieces (Sreejith and Ngoi, 2000). Another way is to make tool materials more refractory or reduce heat accumulation during machining by using e.g. coated HSS, cubic boron nitride, diamond and ceramics.

2.6 Deep hole drilling

Deep hole drilling is defined as a method of drilling holes with length-to-diameter ratio more than 5 times (Zabel and Heilmann, 2012). Tönshoff et al., (1994) pointed out that drilling is one of the most important metal cutting operations among the traditional machining processes, almost arrives at 33% of all metal cutting operations.

The deep hole drilling process is widely used in many engineering applications like manufacturing hydraulic cylinders, automotive industry, medical and biomedical products and aircraft structures (Biermann et al., 2011), and relevant pictures are shown in Figure 2-8. In the aerospace industry, hole quality is very important for its application. Location and size are the two main elements of precision drilling (Richardson and Bhatti, 2001), but roundness, surface finish inside the hole and straightness of the hole should also be taken into consideration. Using a Taguchi method to model surface finish and improve hole diameter accuracy Kurt et al., (2009) regarded cutting parameters and drilling tools as the two main factors which affect drill performance and hole quality.

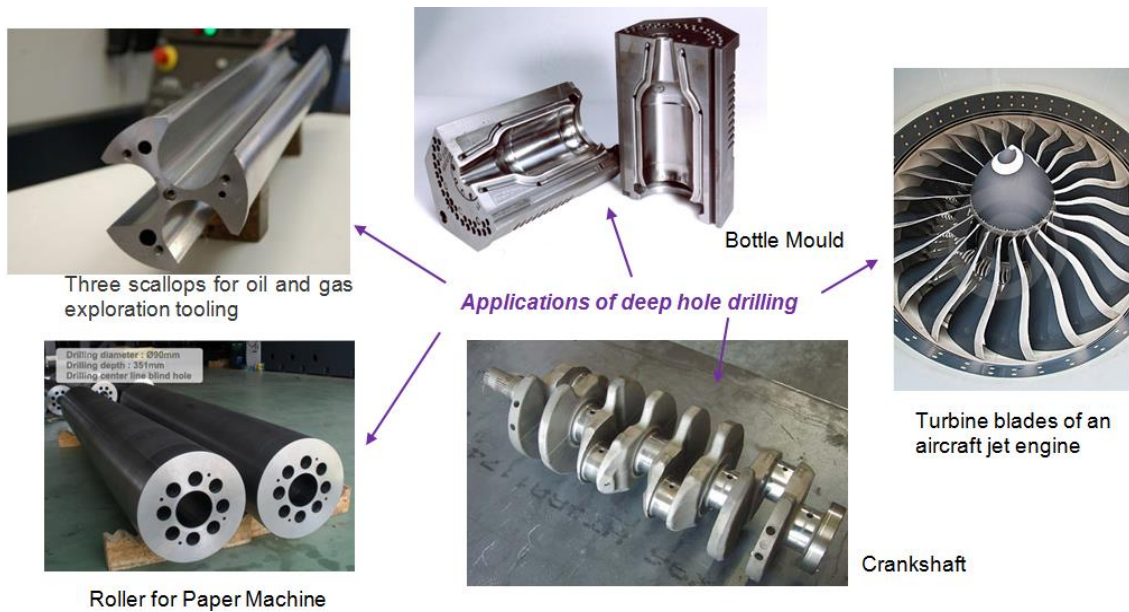


Figure 2-8 Applications of deep hole drilling (Wei Hong co., Ltd)

Nouari et al., (2003) did some drilling experiments about aluminum alloy AA2024 and concluded that raising the helix angle (give an optimal drill geometry), drilling with quite large cutting speed values and weak feed rate, using diamond as coating material can help in achieving a high surface quality and high dimensional accuracy of the holes.

Xavier, L. F. and Elangovan, D. (2013) pointed out that traditional deep hole drilling process can always meet various problems such as tool wear, friction, built up edge and tool deflection which depends a lot on the material being machined. During the drilling process the friction occurred will be able to make the cutting tool edge blurred and finally results tool wear and tool breakage.

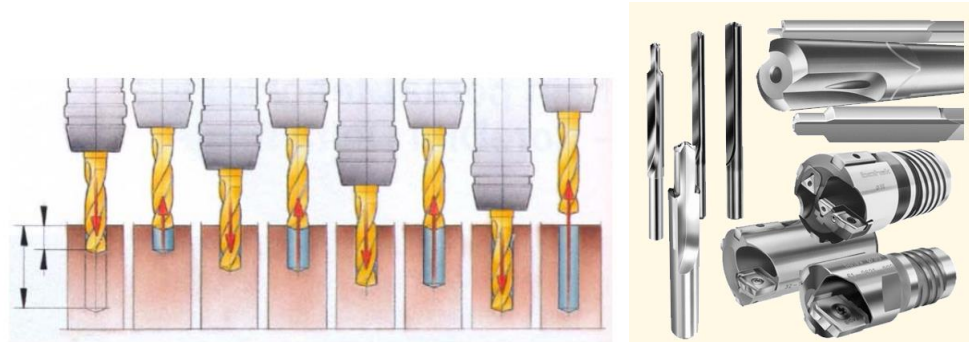


Figure 2-9 Deep hole drilling cycle by traditional drilling tools

Common drills used in engineering are: high speed steel drills (HSS), carbide brazed drills, solid carbide drills, indexable insert drills. Heikki Tikkinen (2010) gave a good way to solve chip evacuation problem of traditional deep hole drilling, after each retrack the hole will be cleaned by cutting fluid and compressed air (see Figure 2-9).

2.7 Research Gap

The following research gaps can be identified from the literature review:

- CMT plus Pulse Advanced is a novel CMT process which can be used to solve the porosity problem associated with the deposition of aluminium alloys. Nowadays, seldom research has been done and articles have been published about this new process of CMT.
- The concept of integration of deposition and milling in one process has been presented by two research groups, but relevant research is still sparse. Further, there is no study of the effect of milling on surface waviness and fatigue life of WAAM structures.
- The deep hole drilling process is widely used in many engineering applications. However, research usually focuses on traditional drilling investigating tool geometry, coating, machining parameters and lubricant impact on the hole quality. No drilling study has been performed investigating small-dimensional deep holes (diameter smaller than 3 mm, length larger than 20mm) using integrated WAAM.

2.8 Summary

The literature review introduced characteristics of Wire and Arc Additive Manufacturing process, methods of integrated deposition and machining process which is also called hybrid-layered manufacturing (HLM) and 3D welding and milling by other research groups, advantages of dry machining compared to conventional wet machining and minimum quantity lubrication machining, features and tools for traditional deep hole drilling.

From the literature review, it can be concluded that the use of Wire and Arc Additive Manufacturing for deposition and milling as a subtractive technique has

many benefits, especially for complex geometrically structures with are hard or impossible to machine the conventional way. As the final WAAM parts should be ready to use, research into the relationship between surface waviness and fatigue life becomes essential. It has also been found from the literature that little attention has been paid to the effect of the milling amount on the WAAM geometry or on stress analysis. No research has been aiming at deep hole drilling utilising the layer-by-layer feature of WAAM.

3 Aim and Objectives

3.1 Aim

The overall aim of this research is to investigate integrated deposition and machining of Al using WAAM process.

3.2 Objectives

The specific objectives of this project are:

- Investigate the integrated deposition and machining of wall structures;
- Investigate the relationship between milling amount, surface waviness and fatigue life;
- Investigate the strategy of applying integrated deposition and machining (milling and drilling) to create deep holes with small diameters (less than 3 mm).

3.3 Project Scope

- The main material used in this research were 4043 aluminium alloy filler, another little part is about mild steel 235. The properties of these two materials are introduced in the Chapter 4. Microstructure studies and mechanical testing are out of scope.
- The machines used in this research are the HiVE machine for deposition and milling, a manual drilling machine. The main machining strategy is dry machining.
- The process is WAAM and the geometry is vertical walls, not inclined walls.

3.4 Methodology

The research methodology consists of four major phases, as illustrated in Figure 3-1. The main tasks and deliverables for each phase are also presented.

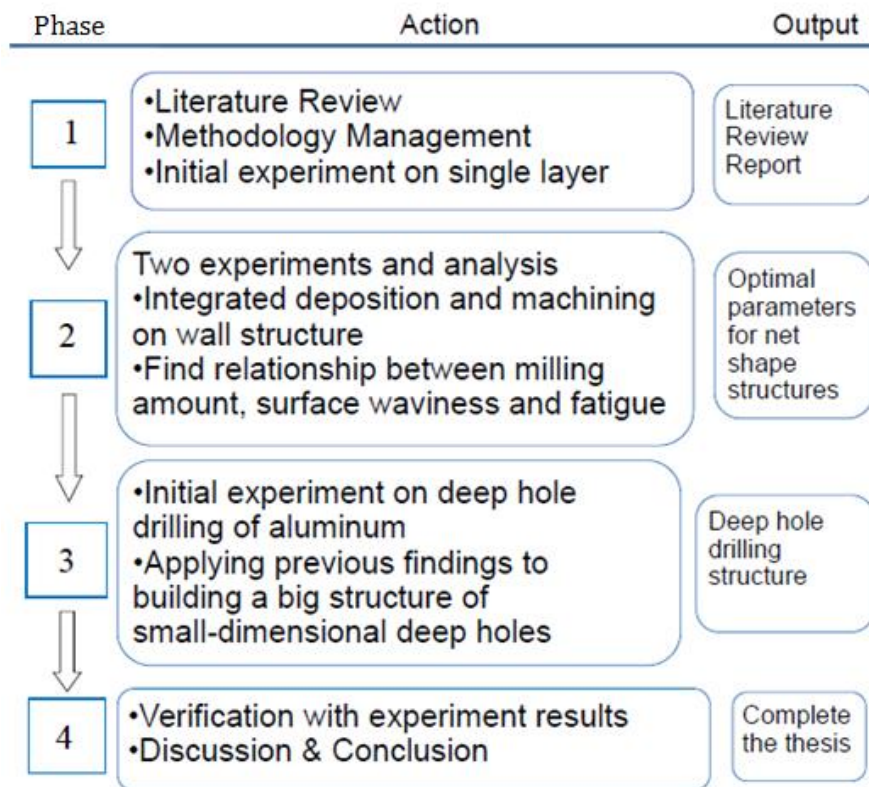


Figure 3-1 Research methodology

3.4.1 Phase 1: Start of the research

The main tasks of phase 1 include good understanding of WAAM process, research aim, objectives and scope of this project, then finding relevant books, journals, website to collect useful articles, scheming time and content for each phase. A literature review is performed with regard to Additive Manufacturing, dry machining, integrated deposition and machining, deep hole drilling. Fundamental experiments for single layer and integrated deposition machining were performed to find reasonable parameters of deposition and milling.

3.4.2 Phase 2: Two experiments and analysis

In the second phase, the integrated deposition and milling process on aluminium alloy was investigated. Experiments were performed with different deposition parameters as well as different milling amounts. The effect of these parameters on the surface finish of the wall was studied. Geometric data, such as wall width, surface waviness, and radius between the subsequent layers

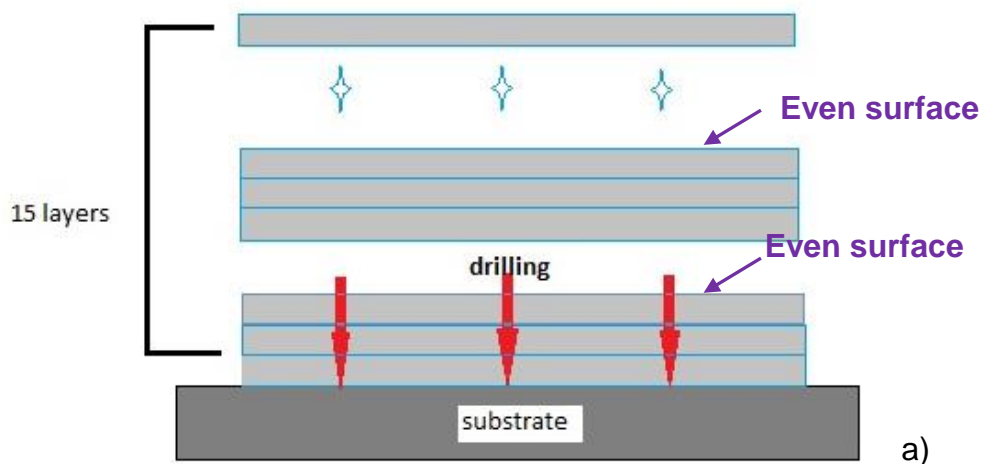
were measured. This geometry data was input into an FEA model for calculating the stress concentration factors. The mechanism of using this integrated process for getting a small concentration factor was discussed. A model was developed to help setting the optimal milling parameters to optimise the quality of the finishing surface.

In addition, experiments on integrated deposition and machining extended to another material, mild steel 235, to see whether it has the same trend of surface waviness, radius and stress concentration factor with the change of milling amount.

3.4.3 Phase 3: Apply integrated deposition and machining process to deep hole drilling

In the third phase, the research was extended to the strategy of using integrated deposition, milling and drilling for making deep narrow hole structures. A large sample was built with multiple deep holes using the integrated process. X-ray inspection was used to check the quality of the holes.

Fundamental drilling experiment were performed on walls were each three layers wide. After milling, a drilling step followed on the now even surface. The milling prevented the drill from slipping from the original circular surface to guarantee the straightness of all consecutive holes (see Figure 3-2).



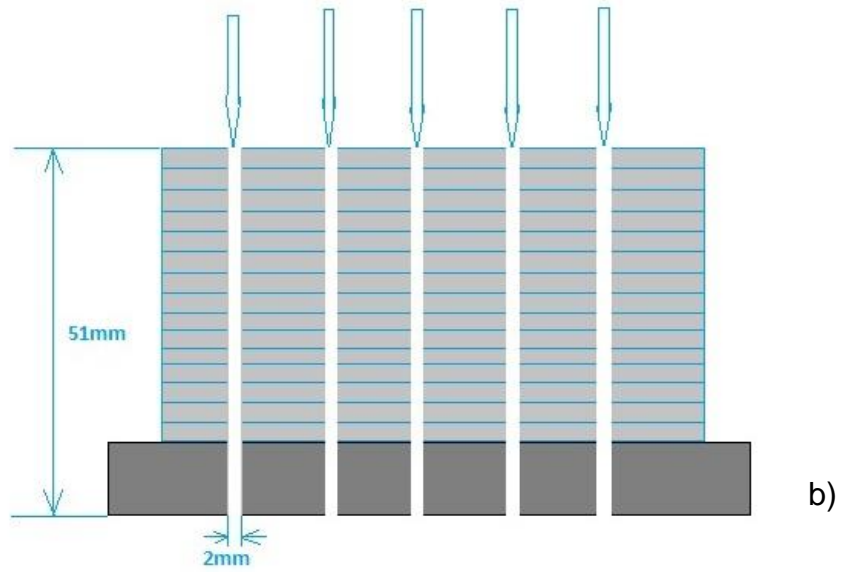


Figure 3-2 Deep hole drilling strategy a) drilling process b) finished sample with some small-dimension holes

3.4.4 Phase 4: Summary

According to the results and analysis, some important conclusions will be got in this phase.

4 Experiment on integrated deposition and machining

4.1 Introduction

This chapter specifies the materials of substrate and wire, dimensions, deposition and machining procedures, measuring method utilised during the research. In addition, corresponding experimental results, discussion and summary of single layer welds and multi-layer welds in aluminium and mild steel are contained in this chapter. Note that main research is focused on integrated deposition and machining on aluminium alloy using WAAM.

4.2 Materials and experiment set-up

The filler wire used in this research is aluminum alloy 4043, with diameter of 1.2mm, composition for 4043 alloy is given in Table 4-1:

Table 4-1: 4043 Alloy Classification Composition Requirement (Weight Percent)

Silicon (Si)	Iron (Fe)	Copper (Cu)	Manganese (Mn)	Magnesium (Mg)	Zinc (Zn)	Titanium (Ti)	Beryllium (Be)	Others Each	Others Total	Aluminium (Al)
4.5-6.0	0.8	0.30	0.05	0.05	0.10	0.20	<0.0003	0.05	0.15	Remainder

According to AWS A5.10 specification, 4043 (Al-5Si) filler metal has the properties of excellent corrosion characteristics, low melting temperature, low shrinkage rate, higher fluidity and hot cracking sensitivity, which makes it a popular aluminium/silicon filler alloy for general purpose deposition applications.

It is specified for many aerospace structural applications, such as fuselage structure, shear webs and ribs and structural areas where requires high fatigue resistance and good strength. Composition for 2024 substrate is shown in Table 4-2.

The substrate used here is aluminum alloy 2024 base plate, the dimension of this plate is 12 mm thick cut into 300mm x 140mm sections.

Table 4-2: 2024 Alloy Classification Composition Requirement (Weight Percent)

Si	Fe	Cu	Mn	Mg	Cr	Zn	Ti	Others (each)	Others (total)	Balance
0.5	0.5	3.8-4.9	0.30-0.9	1.2-1.8	0.1	0.25	0.15	0.05	0.15	Aluminum

The main process used in this project is CMT plus Pulse Advanced (CMT-PADV) which uses reverse polarity to reduce the heat input even further than sole CMT process. When operating with negative polarity, there is more heating in the electrode than in the substrate. This reduces the overall heat input to the weld deposit and minimises dilution. The HiVE machine was used as the motion system (as shown in Figure 4-1a). The HiVE machine is a large gantry system with three main moving axis implemented for large scale WAAM incorporates welding, milling and rolling. The x-axis is the moving bed of the machine and the y and z axes are both on the gantry. The capability of the HiVE machine can be used to fabricate component maximum 3.5 meters long, 2 meters wide and 0.5 meters high.

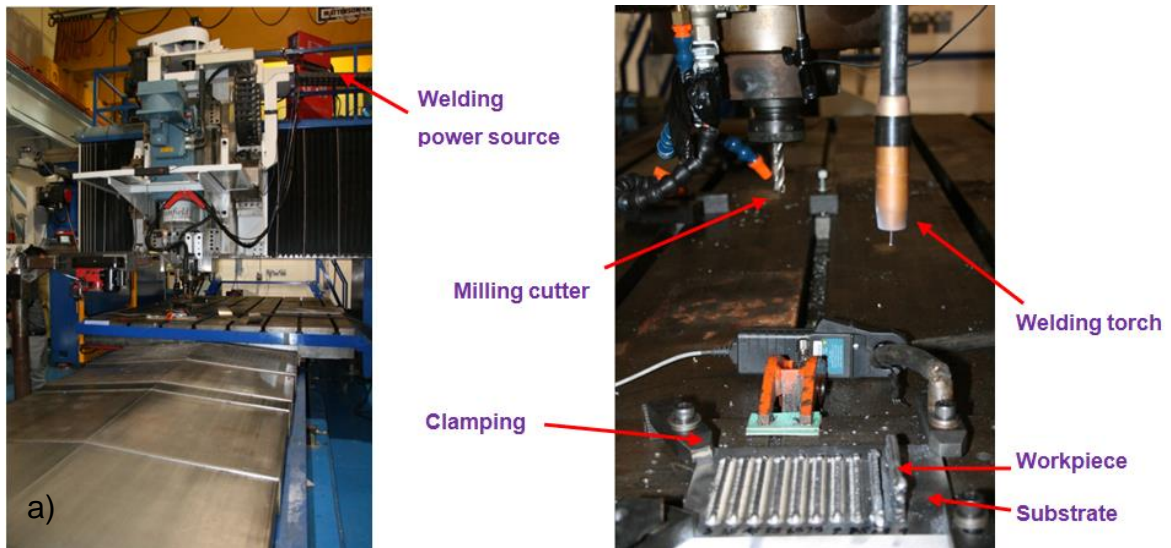




Figure 4-1 WAAM systems: a) HiVE machine b) Control console c) RCU 5000i control pendant

Figure 4-1b) shows the main control console of HiVE machine, suspended from an articulated arm attached to the front of the gantry, houses all the controls used to operate the machine. Figure 4-1c) is RCU 5000i control pendant for setting Wire feed speed and process.

4.3 Fundamental characterization of single layer welds in aluminum alloy

4.3.1 Experimental condition for deposition









These experiments were carried out in accordance with the deposition conditions described in Table 4-3. The 1.2 mm aluminium alloy 4043 filler wire was deposited on 2024 aluminium plates with a special GMAW processes, namely, CMT plus Pulse Advanced (code 1369), which uses reverse polarity to reduce the heat input even further than CMT, with shielding gas 100% Argon. Experiment set-up is shown in Figure 4-1a.

Table 4-3: Experimental condition for deposition of 4043 Al-alloy

Welding Process	Shielding gas	Flow rate (l/min)	Contact Tip Work Distance (mm)	Torch Angle (°)	WD (mm)
CMT-PADV	100%Ar	15	15	90	1.2

The experiments detailed in this section were using CMT-PADV to deposit single weld beads at constant WFS/TS ratios keeping with 15, deposition parameters and bead characteristics are showed in Table 4-4.

Table 4-4 Deposition conditions and bead characteristics of single layer welds

Nominal WFS (m/min)	TS (m/min)	WFS/TS ration	Quality	Picture
3.0	0.2	15	Too narrow	
3.5	0.233	15	Stable	
4.5	0.3	15	Stable	
5.5	0.367	15	Stable	
6.5	0.433	15	Stable	
7.5	0.5	15	Stable	
9.0	0.6	15	Stable	
10.5	0.7	15	Stable	

4.3.2 Results

Relevant parameters of single bead profiles are bead width (W) and bead height (H) in this project. Figure 4-2 indicated the single bead shape which was taken from macro cross sections.

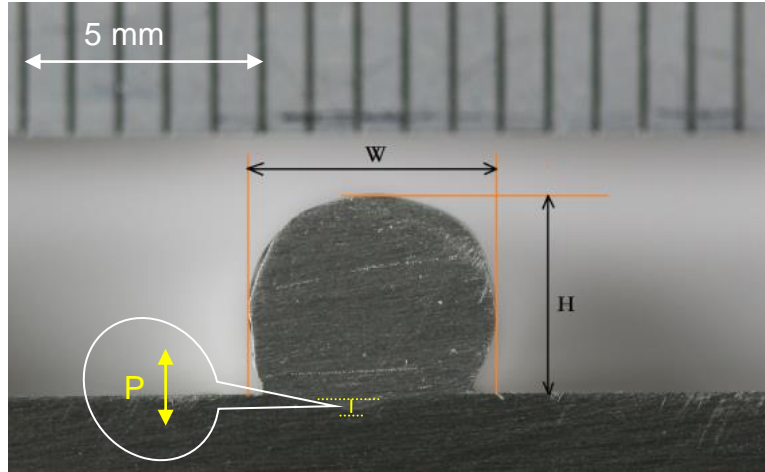


Figure 4-2 Measuring of macrograph single bead transverse with CMT-PADV process, W refers to bead width and H means bead height

Here, the CMT-PADV process was chosen to deposit single weld beads for constant WFS/TS ratio at 15. When the WFS were tried from 3 m/min to 10.5 m/min, the corresponding TS were from 0.2 m/min to 0.7 m/min. From this single layer bead on plate experiment it was hard to conclude which parameters were the optimal in the ranges, because all the layers seemed stable despite the first one was too narrow.

It is shown in Figure 4-3 that bead size heavily depends on WFS and TS. With the increase and decrease of WFS and TS at the same ratio, the width rose from 3.89 mm to 5.65 mm, the height dropped from 5.51 mm to 3.75 mm.

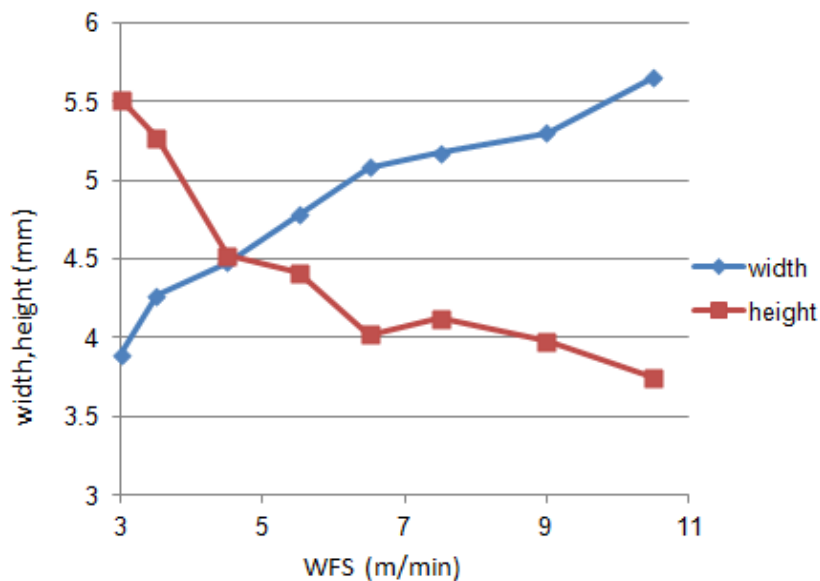


Figure 4-3 Height and width of single beads at different wire feed speeds

4.3.3 Discussion

Penetration is the depth to which the melting take place (see Figure 4-2), the higher the penetration the better is the quality of joint (Karunakaran et al., 2010). Figure 4-4 reveals the macroscopic cross section of single beads, it can be seen that when using the setting WFS at 3 m/min, the bead just had a little connection with the substrate, it seems that the penetration depth was very small (just several micrometres). Spencer et al., (1998) found that complete penetration could be achieved by increasing the current, but this resulted in the loss of bead profile, so this parameter is not suitable in this project.

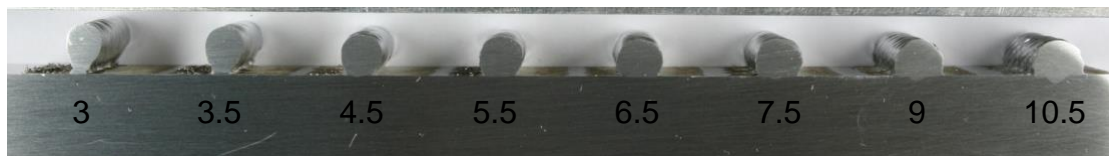


Figure 4-4 Macroscopic cross section of single beads

The result in Figure 4-4 also shows that keeping WFS/TS ratio at a constant value and varying the WFS between 3.5 m/min and 7.5 m/min and TS between 0.233 m/min and 0.5 m/min constitutes an effective approach to control the size and shape of beads. The beads shape can be changed by varying the WFS and TS.

4.4 Experiment of multi-layer deposition in aluminum alloy

4.4.1 Parameters selection and methodology

According to the effect of process parameters on the characteristics of the previous eight single layer welds, subsequent experiments were performed to investigate multi-layer deposition features. This investigation aims at manufacturing multi-layer walls with an identical method to single layer, such as deposition process, shielding gas and constant WFS/TS ratio. Except for the narrowest single weld with 3 m/min WFS, other parameter settings provided stable preference which were selected for multi-layer and integrated deposition with machining experiments, the time interval for cooling between two layers

were set 3 minutes to prevent high temperature results in collapse or other defects of deposited walls. Figure 4-5 a gives the five 10-layer walls with WFS set from 3.5 m/min to 7.5 m/min. Figure 4-5 b shows the experiment set-up for these five walls, c) and d) are 10-layer wall of WFS set at 9.0 m/min and 3-layer wall of WFS set at 10.5 m/min respectively.

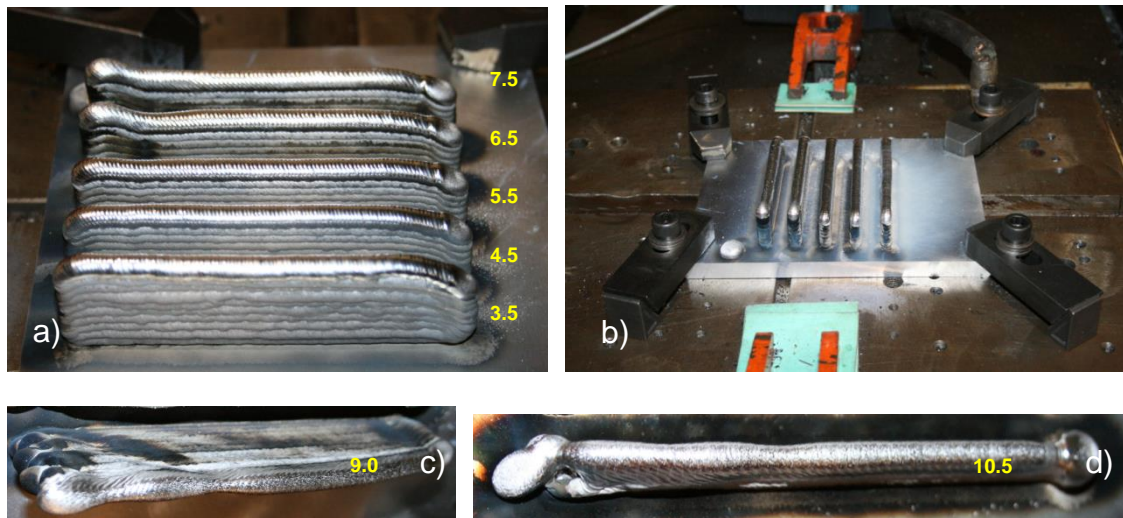


Figure 4-5 a) WFS from 3.5 m/min to 7.5, b) method that substrate clamped on bed for 4 points, c) 10-layer welds with 9.0 m/min WFS and 0.6 m/min TS, d) 3-layer welds with 10.5 m/min WFS and 0.7 m/min TS.

4.4.2 Results

All results presented in this section are according to the experiments detailed in Section 4.4.1. When experiments were extended from single layer welds to multi-layer deposition, it is clearly see from Figure 4-5 a that deposition parameters in the range from WFS 3.5 m/min to 7.5 were suitable for multi-layer walls, however, when WFS 9.0 m/min and 10.5 m/min were applied, the wall were not stable with poor quality, the later one even could not deposited for the fourth layer, because after the third layer it was collapsed from the arcing stage. Thus, only five suitable process parameters would be selected to the following experiment on integrated deposition and machining study.

After that, one experiment was carried out on deposition with top milling at 2 mm fixed height increment for each layer until 10 layers, to see the difference between two kinds of walls with and without top milling. Figure 4-6 a shows the

comparison of the two deposition walls, the above one was deposited layer by layer using WAAM process, the below one was deposited using integrated deposition and machining process, Figure 4-6 b is a cross section of the below wall, from this two pictures it is obviously that face milling affect the geometry of walls a lot, using integrated deposition and machining process has the advantages of controlling the height and surface waviness of structures.

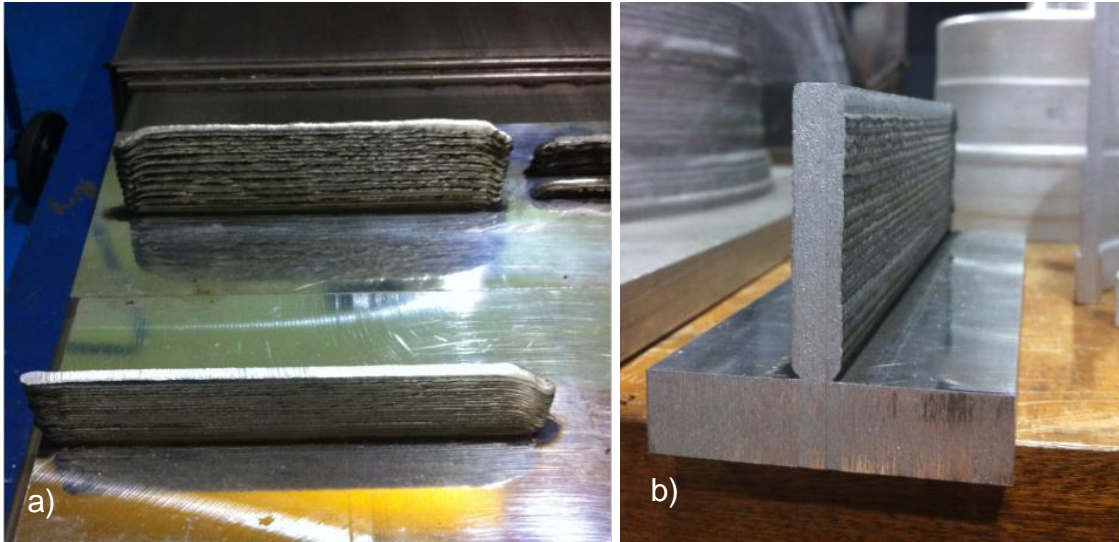


Figure 4-6 a) comparison of the two deposition walls with and without milling, b) cross section of the wall with milling

4.4.3 Discussion

From the results in section 4.4.2, it not only gets the suitable parameters for multi-layer deposition, but also finds that deposition with successive milling step as a cycle process is important and effective procedure. Song et al., (1998) found that the arc welding process can evoke defects in the middle of the layers because of instability, and then small defect will accumulate and affect the height of next deposited bead until no further deposition can be continued. It is concluded that Z direction machining can not only improve the part accuracy, but also make the process more stable for the further deposition. The same as what they mentioned in the article, using WAAM for deposition as the first step, when deposition was done, the instability of the arc deposition process induce flaws in the middle of the weld bead (see Figure 4-7 a). After that, a face milling operation followed as the second step. It was performed to reduce and rectify

the deviation in successive multi-layer deposition and guarantee subsequent deposition could always be applied at a fixed CTWD and smooth surface. Milling the top surface obviously wiped off the oxidized welded surface, as shown in Figure 4-7 b. Regarding the two steps as one circle, then repeated for the remaining layers until a component was obtained.



Figure 4-7 Process principle of integrated deposition and machining, a) WAAM process, b) Face milling process

4.5 Experiment of integrated deposition and machining in aluminum alloy

4.5.1 Experiment

Considering the essential features for some complex components, it is necessary to develop a unique approach that integrates the WAAM process for near-net layer shape and face milling process for net shape. From the initial results in the former experimental development and characteristics of the wall, it is found that integrated deposition and machining process is an effective way to fabricate parts difficult or impossible to be machined.

The experimental setup was the same as the one used for single layer and multi-layer deposition except for adding the milling program in this process. Relevant experimental conditions of deposition are shown in Table 4-3 and suitable parameters of deposition in the range from WFS 3.5 m/min to 7.5 were

chosen from Table 4-4. After the setting operation for deposition was finished, the samples were moved to the position beneath the milling head. After the deposition of one bead the top surface of the deposited layer was machined through planar milling to a desired height for further deposition. Through this step-by-step approach walls with a total height of ten layers were built. Details of the step-by-step technique can be seen in Figure 4-8.

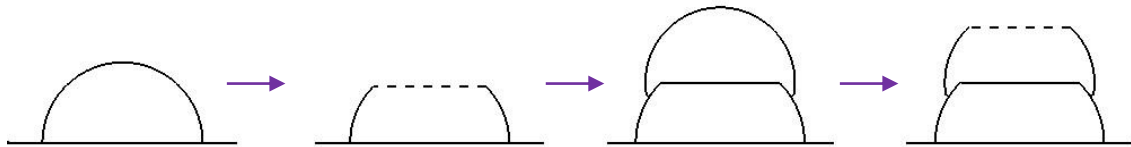


Figure 4-8 Procedure of iterative deposition and face milling

In this project, the prescribed height of each layer of weld walls with WFS set at 7.5 m/min were 2.5 mm by ten layers, 2.0 mm by ten layers, 1.5 mm by fifteen layers, 1.0 mm by fifteen layers respectively, see Figure 4-9. The same prescribed height settings are appropriate for other weld walls with different WFS set here. Milling process was not applied on the top surface of the last layer for all the samples in order to investigate the profile of the bead profile with different WFS set and different milling amount, also data like average layer height, milling amount, remelting area can be measured from the shape of last layer.

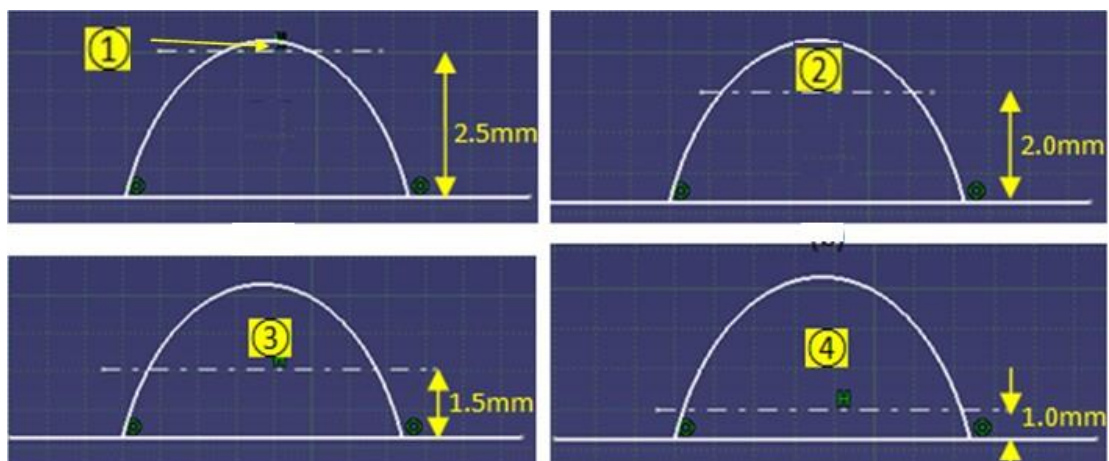


Figure 4-9 Prescribed height for each layer of weld walls

Milling amount is a term in this project that reflects the amount of removed material in the height direction in relation to the average layer height of the

deposited material. As shown in Figure 4-10, H is regarded as the average height of each layer. It is the height that can be measured from the last milling surface to the summit of the wall. m is the depth of cut of one face milling step.

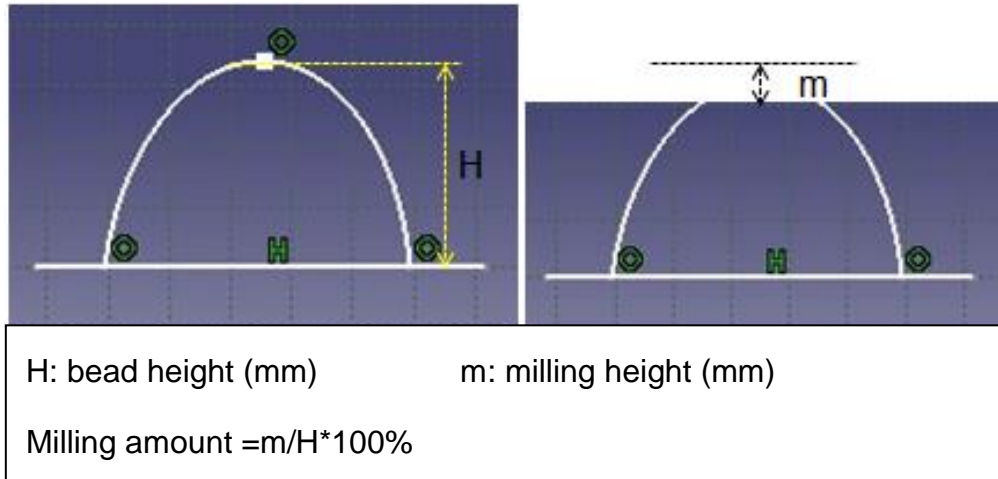


Figure 4-10 Definition of milling amount for multi-layer walls

The milling parameters that used in this research are shown in Table 4-5.

Table 4-5 Suitable milling parameter

Milling speed (m/min)	Feed Rate f (mm/rev)	Machining Process
3.14	60	Dry milling

4.5.2 Results

All results presented in this section are according to the experiments detailed in Section 4.5.1. Note that some detailed data of the results are presented in appendix A with tables and figures.

4.5.2.1 Relationship between deposition parameters and heat input

Heat input is used to measure the relative transferring energy per unit length of each deposition (Chern et al., 2011). According to the average instantaneous power (AIP) method which was proposed by Pickin and Young (2006),

$$AIP[W] = \sum_{i=1}^n \left(\frac{I_i \cdot V_i}{n} \right)$$

Equation 4.1 and Equation 4.2 are used to calculate average deposition arc power and arc energy. An AMV 4000 arc watch system by Trinton Electronics Ltd was used to measure and record the welding current and voltage.

$$AIP[W] = \sum_{i=1}^n \left(\frac{I_i \cdot V_i}{n} \right)$$

Equation 4.1 Average welding arc power

$$\text{Arc Energy}[J/mm] = \frac{AIP[W]}{TS[mm/s]}$$

Equation 4.2 Average welding arc energy

$$HI[J/mm] = \eta \cdot \frac{AIP[W]}{TS[mm/s]}$$

Equation 4.3 Calculation of heat input

Where, AIP [W] is calculated by every the instantaneous current multiply by the instantaneous voltage during deposition for one layer. The arc energy is calculated as the total deposition arc power with the given travel speed. The heat input (HI) is calculated according to Equation 4.3. In addition, a deposition process efficiency factor (η) is usually used to make the heat input more accurate, which depends on the deposition process to a large extent. Sequeira Almeida (2012) recommended the deposition process efficiency factors of $\eta=0.9$ for CMT and $\eta=0.8$ for GMAW-P in the published thesis, so the deposition process efficiency factor was choose $\eta=0.9$ in this work.

The AMV 4000 (see Figure 4-11) is a PC based welding monitor for monitoring data collection for current and voltage through the welding process, help to the calculation of heat input in this project. The heat input (HI) is a quantitative measure of the efficacy of the deposition process and is quantified according to Equation 4.3, specific data is displayed in Table 4-6. It is evident that the shape of weld bead affected by heat input significantly, with the decline of WFS from 7.5 m/min to 3.5 m/min, voltage always maintain at the same level, current decreases from 101.33 A to 67.26 A, average instantaneous power drops from 1335.53 J to 936.93 J, heat input increase fast from 128.2 J/mm to 193.0 J/mm.



Figure 4-11 AMV 4000 machine

Table 4-6 CMT-PADV for deposition parameters and calculation of heat input

WFS [m/min]	TS [m/min]	Voltage [V]	Current [I]	Power [J]	Heat Input [J/mm]
7.5	0.500	13.18	101.33	1335.53	128.2
6.5	0.433	13.38	97.53	1304.95	144.7
5.5	0.367	13.12	88.51	1161.25	151.9
4.5	0.300	13.49	81.93	1105.24	176.8
3.5	0.233	13.93	67.26	936.93	193.0

4.5.2.2 Effect of milling amount on Effective Wall Width (EWW) and Surface Waviness (SW)

Considering that the first four layers are not steady because of the cold substrate, the measurement of EWW and SW started from the fifth layer of the deposited wall. The EWW parameter refers to the final effective wall width accomplished by post-processing milling or dimensions acquired by machining steps to net shape. The SW defines the irregularities area which occurs suddenly in a relatively flat surface, it is used to indicate the surface quality of multi-layer wall. CATIA software was used to measure the SW in this research.

SW was determined by distance from peak to valley and then the average data from both side of a wall was calculated (see Figure 4-12).

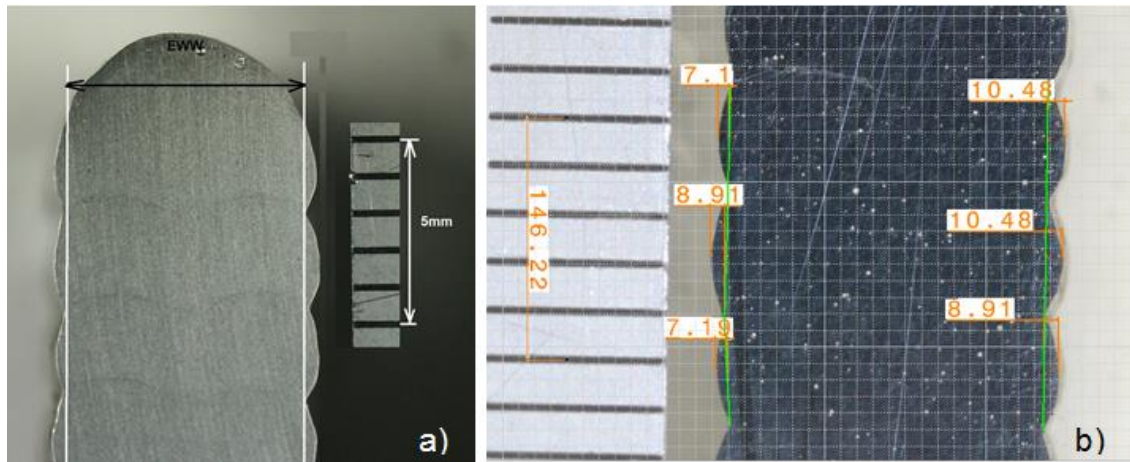


Figure 4-12 a) Method for measuring effective wall width, b) Method for measuring surface waviness

In this section, the effect of milling amount on SW and EWW of multi-layer weld bead characteristics are presented. Multi-layer with 10 and 15 layers high were produced according to the deposition conditions detailed in Section 4.2.4. Figure 4-13 depicts the cross-sectional macrographs of SW and EWW in the condition of different milling amount. It is apparent that milling amount has positive effect on reduction of SW and EWW, SW decreases and EWW increases as milling amount increases.

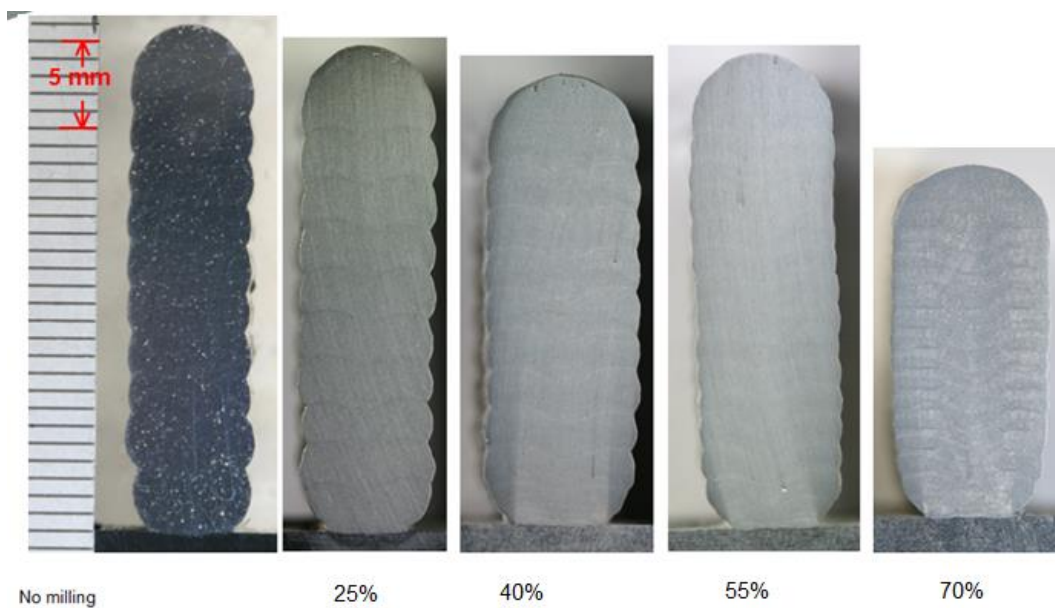


Figure 4-13 Cross-sectional macrographs of deposition welds with different milling amount

The effect of milling amount on EWW is shown in Figure 4-14 for constant WFS/TS ratio conditions. All five groups have the similar trend that EWW increase with the growth of removal milling amount. It is evident that the growth of removal milling amount has positive and significant effect on EWW when WFS set at 7.5 m/min and 6.5 m/min, whilst small effect was observed when WFS set at 3.5 m/min.

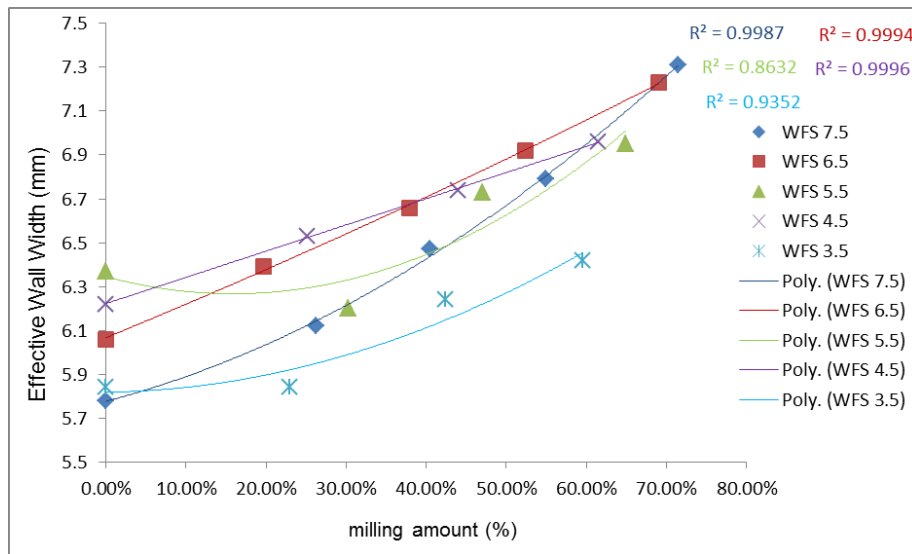


Figure 4-14 Polynomial trendline of scatter charts about relationship between milling amount and effective wall width at constant WFS/TS ration

The polynomial trendline of scatter charts shows the relationship between surface waviness and milling amount (see Figure 4-15), it can be seen that the five groups have the similar trend, surface waviness decreases with the increase of milling amount, more specifically speaking, all the five groups can get very small surface waviness (less than 0.1 mm) when milling amount arrives at 60% to 70.

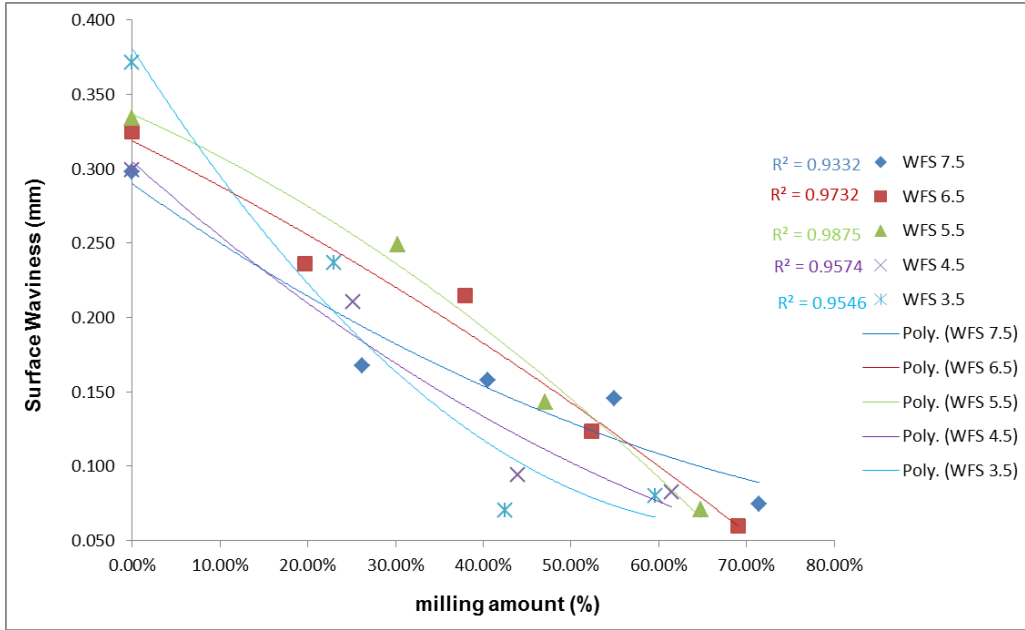


Figure 4-15 Polynomial trendline of scatter charts about relationship between milling amount and surface waviness

4.5.2.3 Effect of milling amount on Material Efficiency in aluminium alloy

Material Efficiency (ME) reflects material utilization compared by those fabricated with traditional WAAM process and integrated deposition and machining process. The ME parameter measures the material utilization factor associated with the AM technique in percent. It is always measured from the last six layers as seen in Figure 4-16.

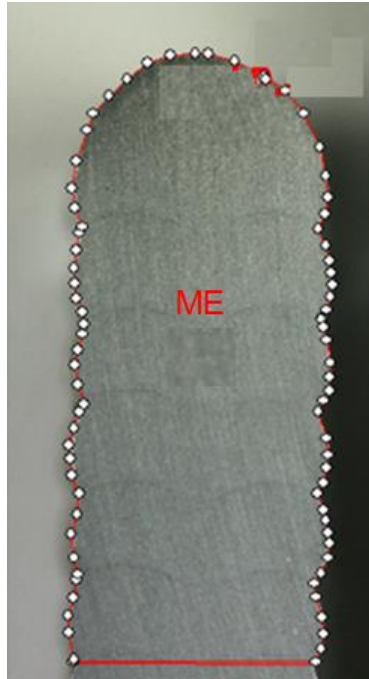


Figure 4-16 Method for measuring the deposition efficiency

This section reports the results of Material Efficiency (ME) in aluminium walls for different milling amount. Deposition conditions are described in Section 4.2.4. Figure 4-17 shows the relationship between milling amount and Material Efficiency, for a range between 3.5 m/min and 7.5 m/min WFS set at the constant WFS/TS ratio. When the milling amount is in the interval no milling to approximately 65%, most groups reflect a linear decline trend of ME from 100% to about 50%, however, the effect of the milling amount on material efficiency is relatively higher when WFS set at 7.5 m/min, compared to those WFS set is from 3.5 m/min to 6.5 m/min. It shows that ME decreases from 100% to about 30% when milling mount increases to 70%, nearly one third of those without milling.

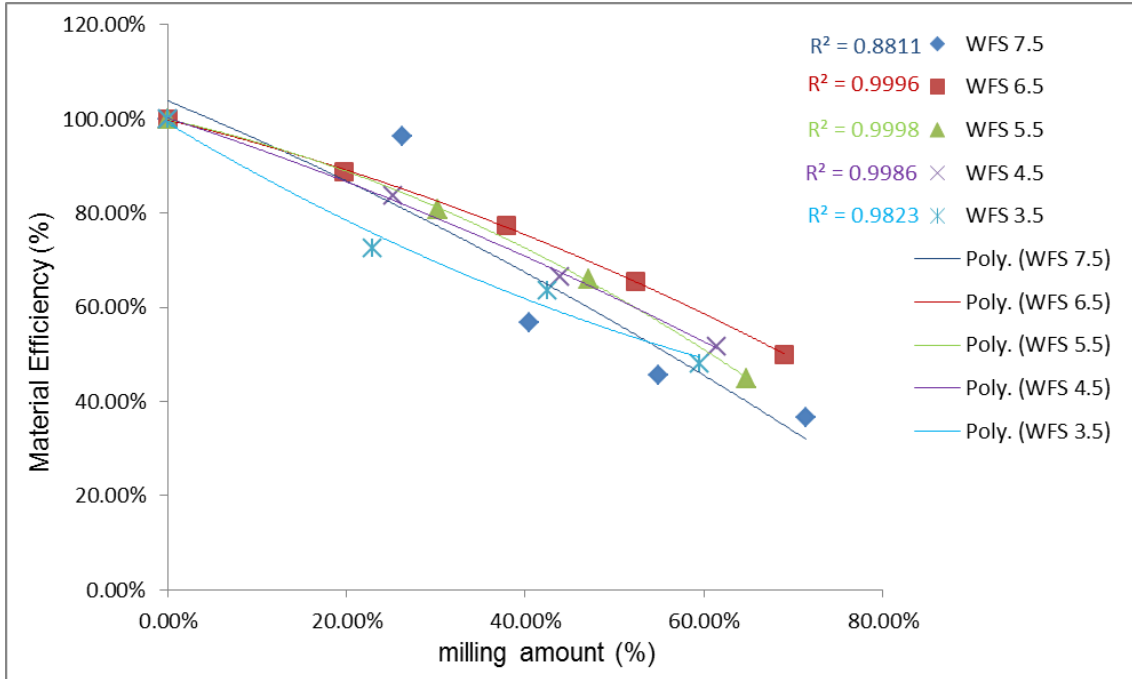


Figure 4-17 Polynomial trendline of scatter charts about relationship between milling amount and Material Efficiency

4.5.2.4 Effect of milling amount on notch radius

Notches are abrupt geometrical changes of a component which is inclined to cause local stress concentrations and thus may induce premature defects (Rösler et al., 2007). It is a significant parameter for the stress concentration, which decides the degree of stress concentration. CATIA software was used to find three points for Bresse normal circle and get the radius between two layers (see Figure 4-18), measuring both sides from the fifth layer to the seventh layer and calculating the average value from these six data points.

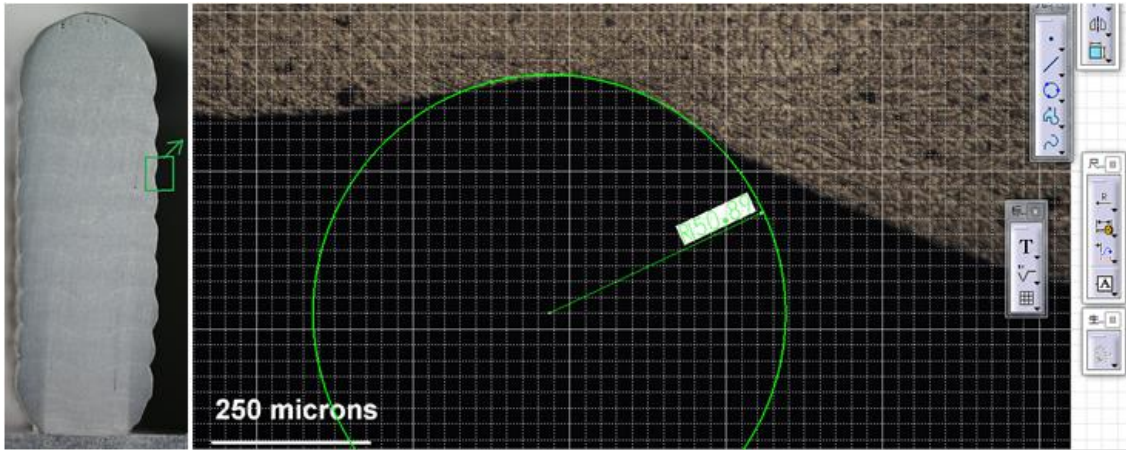


Figure 4-18 Measuring of the notch radius

The scatter chart (Figure 4-19) illustrates that the notch radius can be dramatically increased from no milling to milling amounts arriving at 60% to 70%. However, when the milling amount is lower than 40%, the influence on the notch radius is insignificant. Meanwhile, the scatter chart also shows that the notch radius increases significantly with WFS set at 5.5 m/min, 4.5 m/min and 3.5 m/min, respectively. The effect of milling amount on the notch radius is relatively small when WFS is 7.5 m/min and 6.5 m/min.

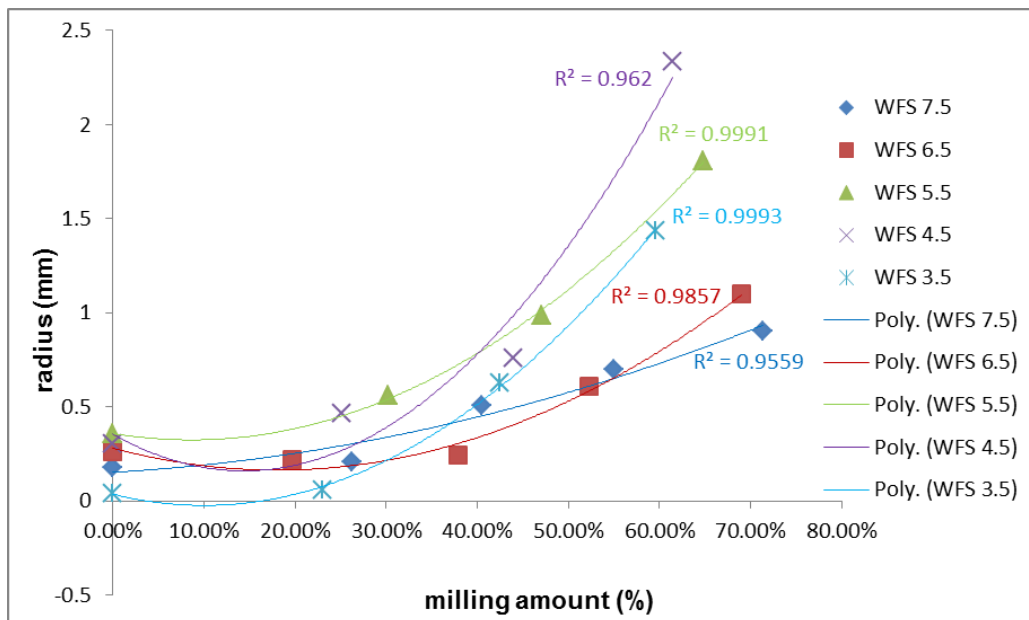


Figure 4-19 Polynomial trendline of scatter chart about relationship between milling amount and notch radius

4.5.2.5 Effect of the milling amount on the stress concentration factor

In order to calculate the stress concentration factors in the notch region, a two-dimensional FEA model was developed using the software Abaqus 6.11-2. A script was developed to determine the model efficiently. A 20-layer wall was built for each sample. Parameters such as layer height, waviness, layer width, and notch radius were used as the input to this model. Constant elastic properties were used in this model. The Young's Modulus was set to 76GPa, and the Poisson's ratio was set to 0.34. Uniformly distributed stresses with magnitude of 100MPa were utilised on the two ends of the wall. The directions of the stresses on the two ends were opposite along the y-direction. To capture the rapid stress increase around the notch radius, smaller elements were utilised in these areas.

Figure 4-20 shows a section of WAAM wall around a notch. It can be seen that the stress magnitude increases in the region of the notch (shown in red), which could become a potentially critical stress raiser in the component.

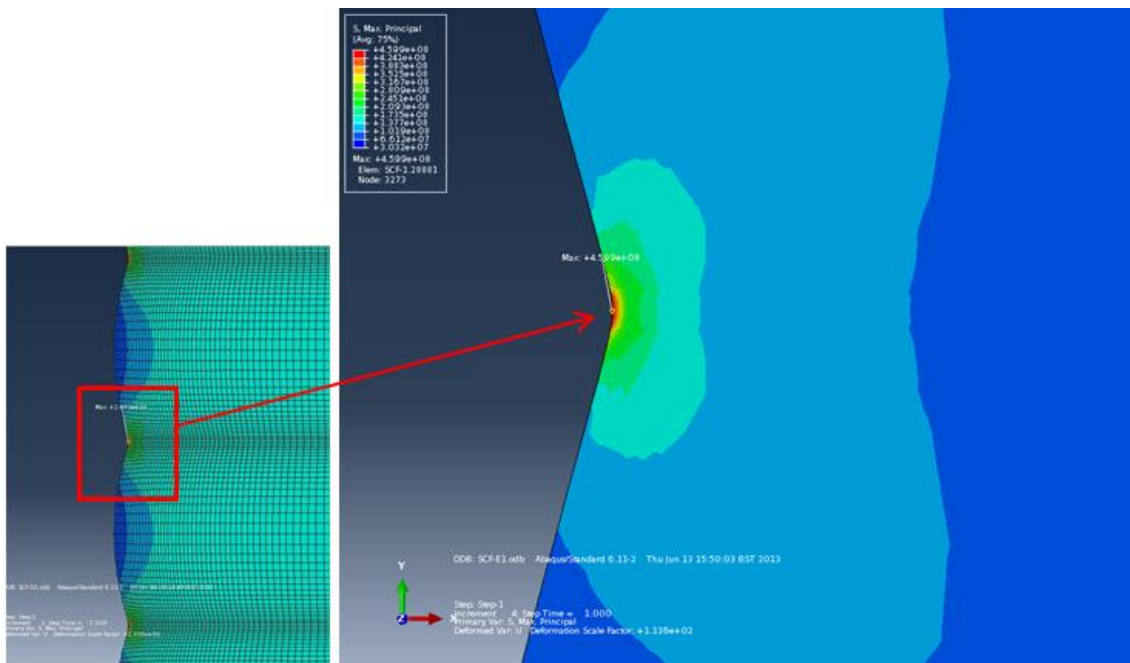


Figure 4-20 Stress concentration factor predictions from FEA model

From Figure 4-21, it is apparent from the information supplied that when the milling amount reaches 60% to 70%, all five groups with fixed WFS/TS ratio can

reach significantly small stress concentration factors close to 1, i.e. the optimal condition for long fatigue life.

After analysis and comparison, it was found that the notch radius and surface waviness have a critical effect on the stress concentration factor. Smaller stress concentration factors can be achieved through larger notch radii and smaller waviness. When the milling amount arrives at an optimal level, a near-net shape or even net shape surface with minimal stress concentration factors can be reached.

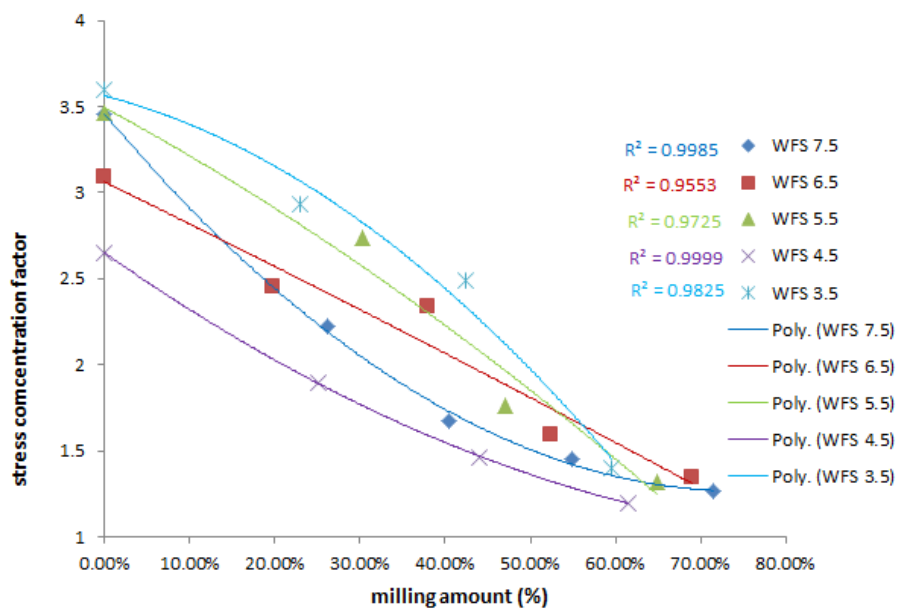


Figure 4-21 Polynomial trendline of scatter charts about relationship between milling amount and stress concentration factor

4.5.3 Discussion

4.5.3.1 Analyse factors that have effect on geometry

The objective of this study is to investigate the relationship between the milling amount, surface waviness with fixed WFS, TS and constant WFS/TS ratios were employed. This section is focused on the discussion of the relationship between milling amount and surface waviness. According to the results in section 4.3, it is found that deposition parameters and milling amount play crucial roles that determine the geometry of the final wall. They affect the shape

of the weld bead and the covering form of the later layer to the former layer respectively.

a) Deposition parameters

In this project, W and H were used to describe the weld bead in single layer welds, whilst the EWW, SW, notch radius and ME were utilised to describe features in multi-layer walls. From the results described in the previous section it was found that the deposition parameters are important criteria in determining the shape and dimensions of the weld beads, at the same time influencing the surface finish of the component. Figure 4-22 shows the shape of last-layer of the multi-layer wall samples with different WFS from 7.5 mm/min to 3.5 mm/min at constant WFS/TS ratio. It is evident that the shape of weld beads changes a lot with different WFS, from vertical ellipsoid to horizontal ellipsoid shape. The bead width increased and the bead height decreased with the decrease of WFS.

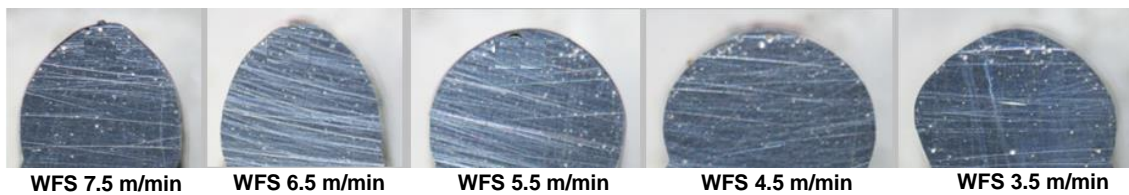


Figure 4-22 the shape of last-layer weld bead of multi-layer with different WFS from 7.5 mm/min to 3.5 mm/min at constant WFS/TS ratio

Figure 4-23 shows the different wave form from different processes, one was from CMT plus Pulse Advanced process, the other was from CMT process, and obviously Heat Input with CMT plus Pulse Advanced process is lower than CMT process.

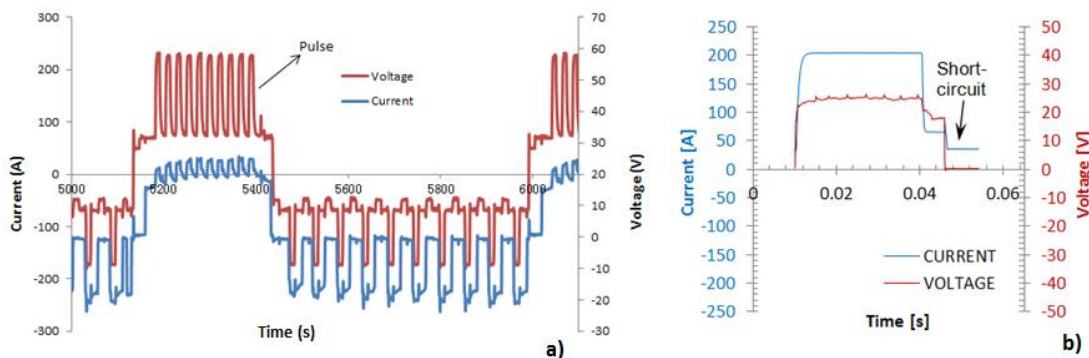


Figure 4-23 Current and voltage in same welding parameters: a) Wave form of the CMT-PADV process for multi-layer welds in this project, b) Wave form of the CMT process for multi-layer welds (Cozzolino, 2013)

b) Milling amount

Another factor that affects the geometry is the milling amount. Because the form of successive deposition covers the former one is different with change of milling amount. ①②③④ in Figure 4-9 refers to the different milling amount (height amount) for each layer, the calculation method is introduced in Section 4.2.5.2, surplus height is controlled by milling tool. Sketch of samples with possible overlap form that the later layer covers the former one is established according to the real shape of samples with different deposition parameter and milling amount. The left picture in Figure 4-24 shows the sample with WFS at 7.5 m/min and small milling amount, the later bead deposited on the smooth surface. When the new layer of material deposited on the already existed layers, the previous layer was partially remelted on the top area. Thus the newly deposited layer slightly covered the previous layer and generated a notch with a sharp angle on the interface between the two layers. Turn to the right picture in Figure 4-24, it shows the sample with WFS at 3.5 m/min and a larger milling amount. In this case the interface between the newly deposited layer and the previous layer was located near the base of the previous layer where the profile of the bead is close to vertical. Thus, the wall was produced with smooth side surfaces.

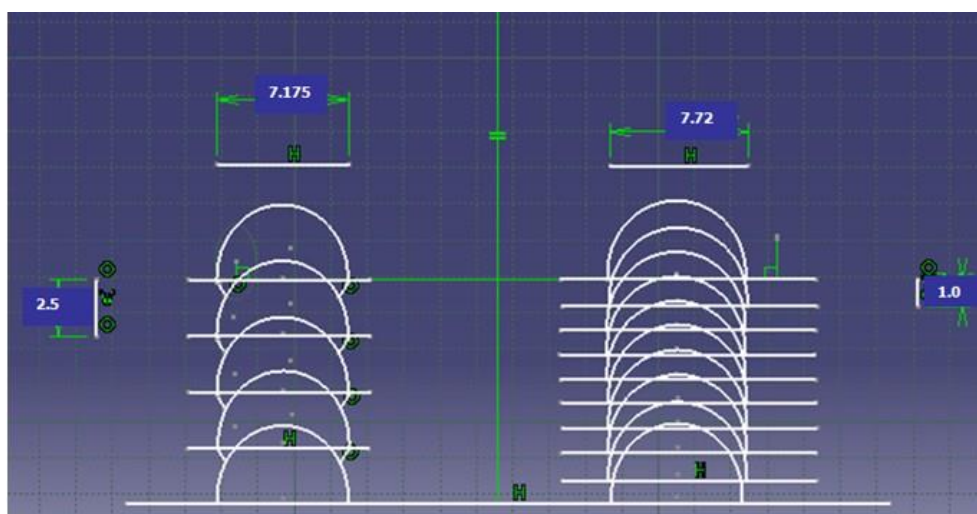


Figure 4-24 Sketch of samples with different overlap forms

The term of Remelting Area (RA) in this project refers to the area of the former deposition which was remelt by the subsequent layer deposition. The layer number of the wall was defined using 'x'. WH is the total height of these x layers. HH is the height from the substrate to the last face milling surface. All the data were taken from the multi-layer cross sections, as indicated in Figure 4-25.

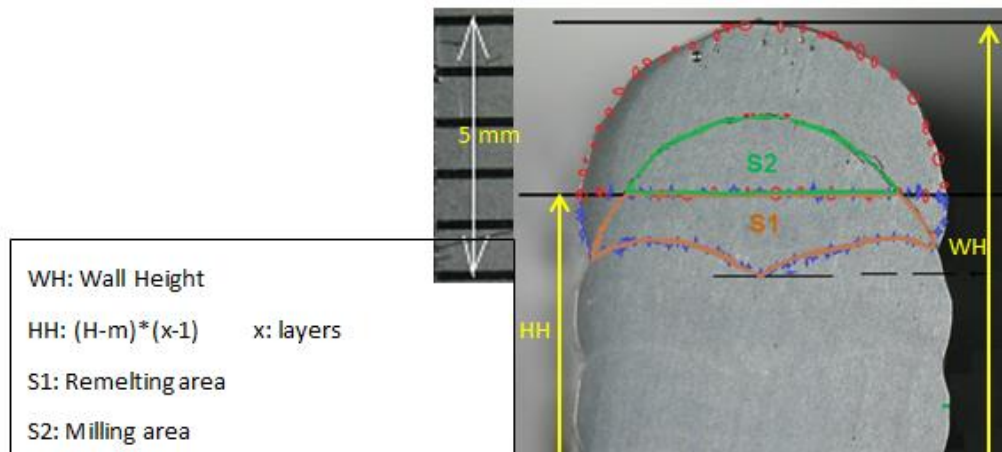


Figure 4-25 Definition of macrograph cross section on multi-layer wall

During the deposition process, after completing the first level, the deposition of the second layer always forms on the track of an existing surface. According to the overlap shape and the remelting area, an ideal model is established to estimate the optimal milling amount for minimum surface waviness.

Figure 4-26 b shows the ideal model. First the following hypothesis is introduced: the cross-sectional area of each layers are the same, ignoring the impact of heat input on the shape of layer. When the subsequent layer deposited on top of the previous layer, the top of the previous layer was remelt. The height of the remelt area determines the position where the new layer starts (as indicated with Line CD in Figure 4-26 a). To get a flat side surface finishing, the layer boundary position need to be controlled by using a proper milling amount (as shown in Figure 4-26 b).

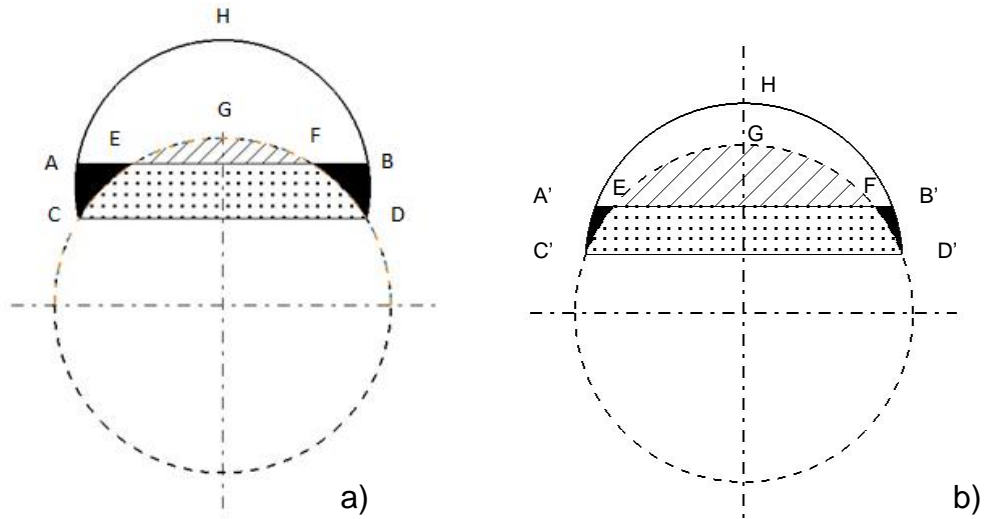


Figure 4-26 Ideal model for overlap form

Using the group WFS set at 7.5 m/min for example, the area of EC'D'F can be measured by Axio Vision software, see Table 4-7.

Table 4-7 Measuring of the remelting area

E'CD'F (mm ²)	EFG (mm ²)	A'C'D'B' (mm ²)	A'B'H (mm ²)
6.32	4.25	7.62	18.43
7.56	4.28	8.57	16.04
4.38	10.32	4.67	20.08
3.27	13.75	3.29	19.33

In fact, the area of ECDF changes significantly according to the actual area.

4.5.3.2 Benefits of using an integrated deposition and machining process

a) Geometry control

Because of the characteristics of integrated deposition and machining process, the milling step can control the height of each layer accurately thus keeping a constant CTWD through the fabrication of the wall. Figure 4-27 shows a sample keeping a 2 mm height for each layer and a total height of 118 mm. As the new layer is always deposited on top of a flat surface, the deposition process is steady. Figure 4-27 b shows the geometry control for both sides, according to

the foregoing discussion, when choosing a reasonable deposition parameters and milling amount arrives at an optimal condition, using the integrated deposition and machining process can make the both sides of structure as net-shape surface.

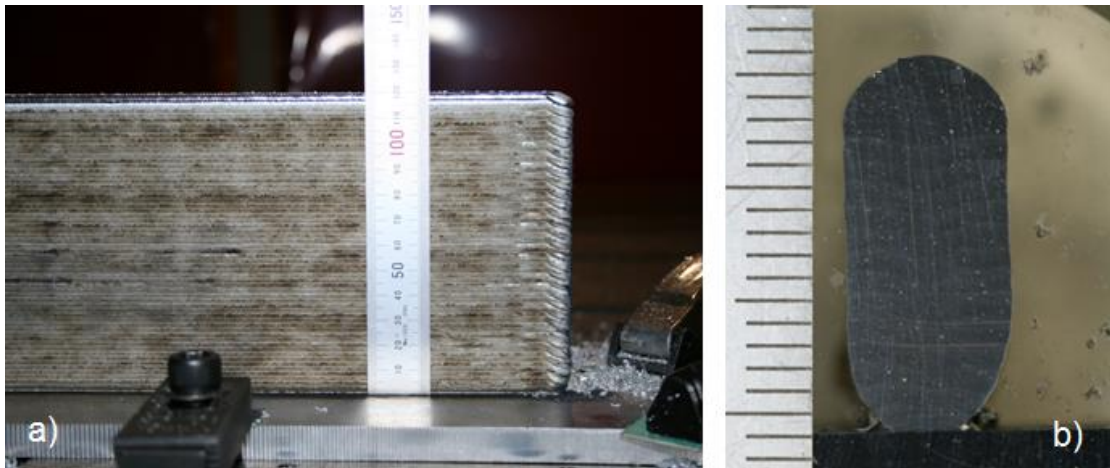


Figure 4-27 Geometry control by integrated deposition and machining process

b) Wall with prolonged fatigue life due to a smooth surface

From the results in section 4.3.3, the notches on the side surfaces of the wall behave as stress raisers, where is prone to promote the initiation and spread of the fatigue process. If the stress in this position is acceptable, the whole structure can meet requirements of tensile properties. It is clear to see that when the milling amount is approximate 60% and 70%, samples can reach a very small surface waviness and a rather large notch radius, thereby significantly reducing the stress concentration factor. It is proved that using integrated deposition and machining process is beneficial to prolong fatigue life.

4.5.3.3 Help to reduce the big porosity on top surface

It is widely recognized that hydrogen is the dominant cause of porosity in aluminium alloy welds (Da Silva, Celina Leal Mendes and Scotti, 2006). Several investigations have shown that porosity plays the prominent role acting as an underlying crack initiation process (Donlon et al., 1996; Mayer et al., 1999). Praveen and Yarlagadda (2005) concluded that the solubility of hydrogen is higher in the liquid stage than in the solid stage (see Figure 4-28). They also

pointed out that entrapped gas in the weld such as shielding gases, impurities, air or water are the main sources of hydrogen in the weld, which occurs due to large difference in solubility of hydrogen in liquid and solid aluminium.

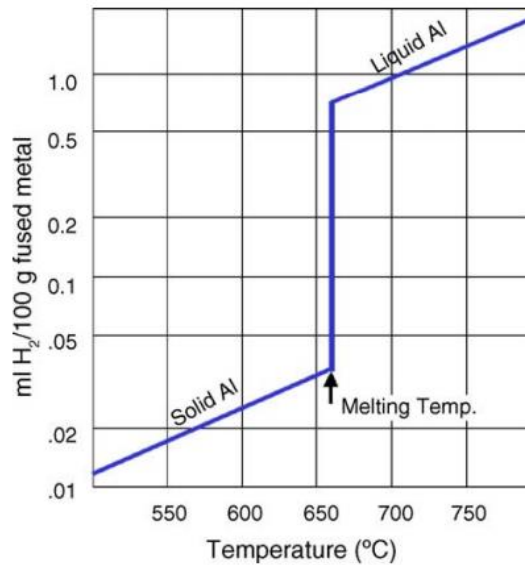


Figure 4-28 Solubility of hydrogen in aluminium at various temperatures (Richard, 1995)

Porosity can significantly reduce the mechanical performance of the aluminium WAAM parts. Through the comparison of some samples using WAAM without milling and integrated deposition and machining process, it is found that the latter process effectively reduces the quantity and size of porosity, especially for the top surface.

Figure 4-29 a shows longitude surface for samples where a traditional WAAM process was used. Figure 4-29 b shows scanning electron micrographs, successively from bottom to top of the sample. It is clearly that there are so many gas pores in each micrograph, especially the one on the top surface with remarkably intensive and big sized gas pores.

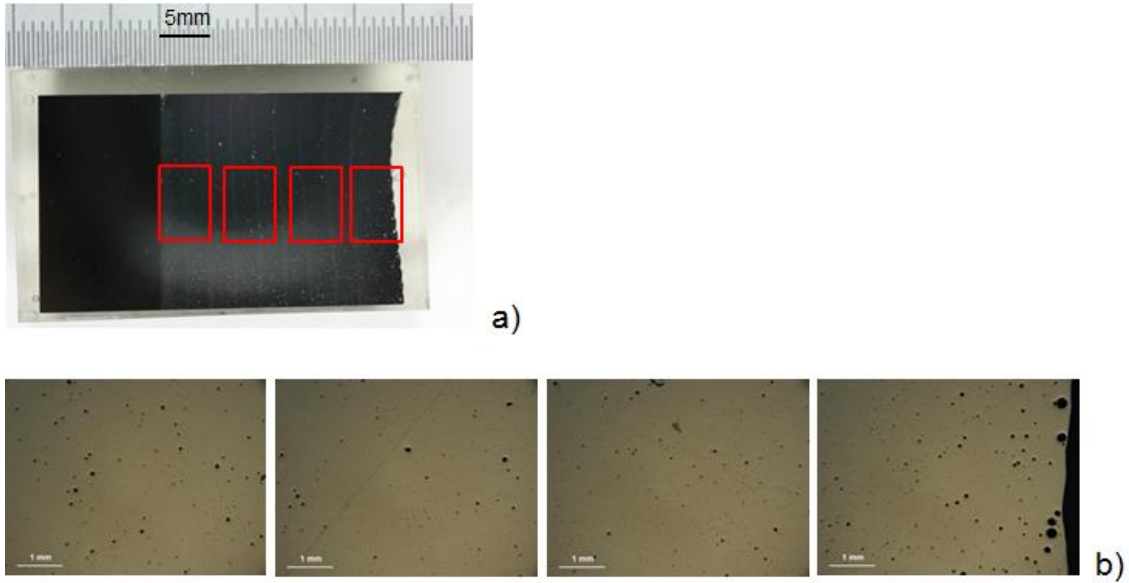


Figure 4-29 Scanning electron micrographs of longitude surface for sample with traditional WAAM process

When using integrated deposition and machining process, the serious gas porosity problem has prominent improved. As shown in Figure 4-30, much fewer gas pores can be observed compares to those in Figure 4-29. During the deposition process, gas pores generated in the melt pool. The pores grow up when they float up to the top surface. Some of the pores cannot overflow from the top surface before the material solidified, which result in big pores near the top surface of the wall. In the subsequent milling step the already generated pores can be removed. Moreover, the milling process removes the oxidised surface which further reduced the porosity.

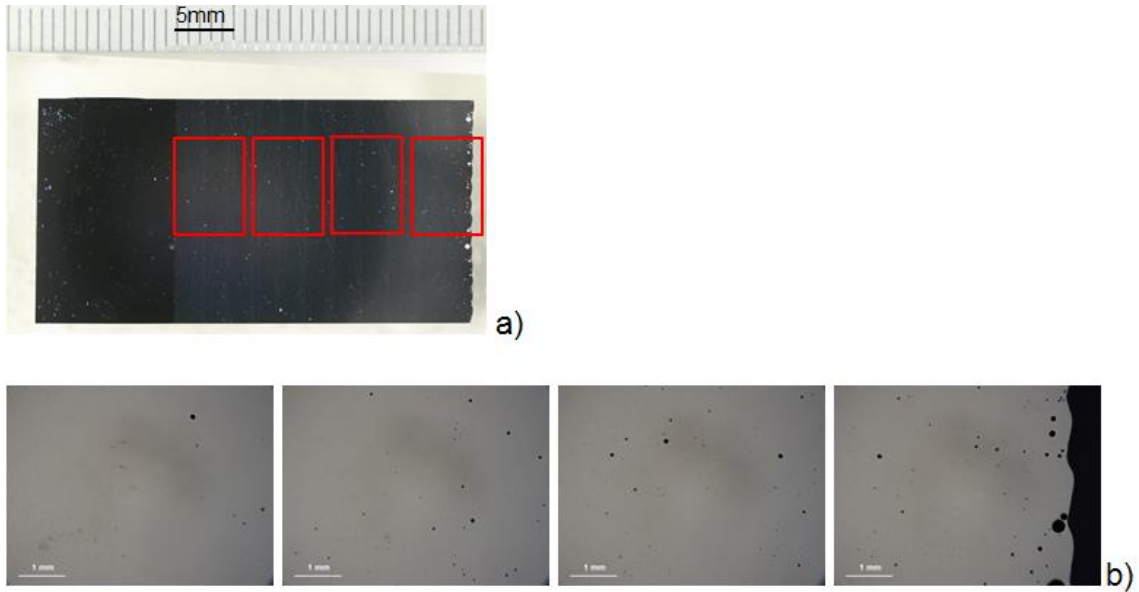


Figure 4-30 Scanning electron micrographs of longitude surface for sample with integrated deposition and machining process

4.6 Experiment of integrated deposition and machining extended to mild steel

4.6.1 Experimental Setup for WAAM on mild steel

The filler material used in this section is mild steel S235, it is one kind of Carbon Manganese steel which is widely used in industry. Substrate material used here is mild steel plates S355, the chemical compositions of these materials are presented in Table 4-8, which conforms to EN 440.94 and BS EN 10025-4:2004.

Table 4-8 Chemical compositions of the mild steel substrates and solid wire electrodes (Weight Percent)

	C	Si	Mn	P	S	N	Cu	Ni	Mo	Al	Ti+Zr	Fe
plate	0.20	0.55	1.60	0.025	0.025	0.012	0.55	0.05	-	-	-	balance
wire	0.06 0.14	0.70 1.00	1.30 1.60	0.025	0.025			0.15	0.15	0.02	-	balance

Deposition parameters were selected in this project based on research of Sequeira Almeida (2012), it has been proved that these parameters were stable and suitable for depositing 1.0 mm diameter mild steel. See Table 4-9.

Table 4-9 Deposition parameters of CMT for mild steel

Nominal WFS (m/min)	TS (m/min)	WFS/TS ratio	layers
7	0.467	15	10
6	0.4	15	10
5	0.333	15	10
4	0.267	15	10
3	0.2	15	10

These experiments were implemented in accordance with the deposition conditions depicted in Table 4-10. CMT process was employed to deposit 1.0mm S235 wire on S235 structural steel with a shielding gas mixture containing Ar/CO₂ (18%).

Table 4-10 Experimental condition for depositing mild steel S235

Deposition Process	Shielding gas	Flow rate (l/min)	Contact Tip Distance (mm)	Torch Angle (°)	WD (mm)
CMT	Ar/CO ₂ (18%)	15	12	90	1.0

Experiment set-up in this section for mild steel is similar as which is for aluminium 4043, except the only difference is that machining process is accompanied with compressed air for cooling equipment. Experiment set-up can be seen from Figure 4-31.

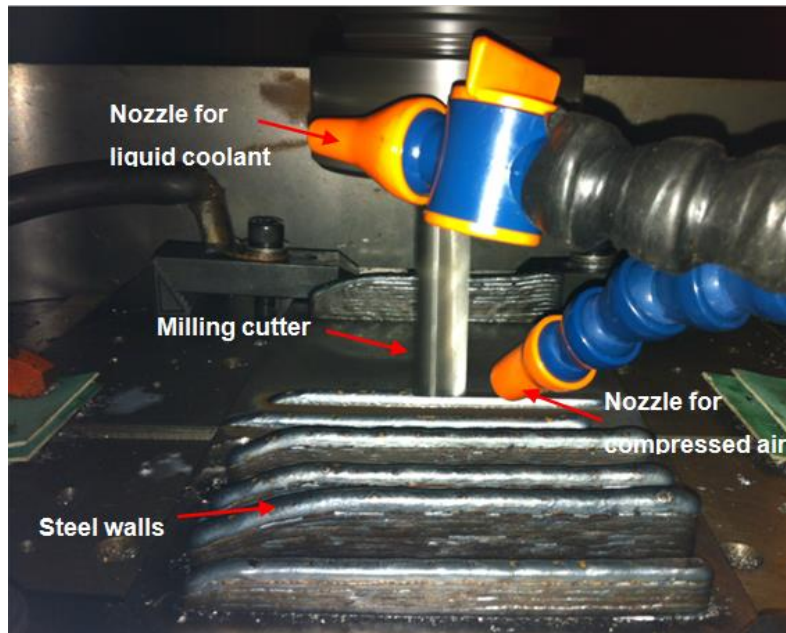


Figure 4-31 Experiment set-up for experiment on mild steel

4.6.2 Measurement of the weld characteristics

The measuring method of surface waviness on steel is different from aluminum alloy because of its illegible boundary, it is assessed using confocal laser scanning microscope, as shown in Figure 4-32.



Figure 4-32 Confocal laser scanning microscope

Confocal laser scanning microscope was used to precisely record surface profiles of each individual sample with 3D images in a setting region. From Figure 4-33 it is seen that one cross profile for each sample is magnified and scanned by 10 times magnifying lens in this scanning with 5 μm for every step increment along the profile. In consideration of time saving, the data was just collected from one side of each sample to represent for both facets.

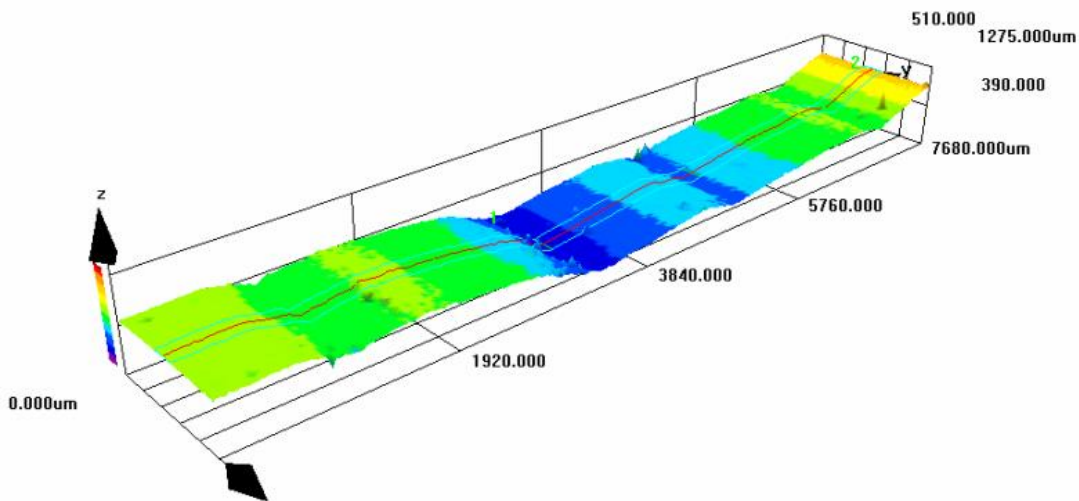


Figure 4-33 3D scanning view which records the contour curve between maximum data from peak and minimum data from valley in a setting region

The SW was determined between maximum data from peak minus minimum data from valley and calculates the average number to obtain representative data, usually 8 points are scanned for each sliced profile in this project.

4.6.3 Results

4.6.3.1 Effect of milling amount on Effective Wall Width

In this section, the effect of milling amount on Effective Wall Width (EWW) for mild steel multi-layer weld bead characteristics is presented. Walls with 10 layers high were produced according to the deposition conditions detailed in Section 4.4.1. It is apparent from Figure 4-34 that effect of milling amount on EWW is negative when milling amount is from no milling to 50%, EWW presents the slightly go down from about 5.5 mm to 5.4 mm, then it jumps dramatically to 6.1 mm when milling amount is from 50% to 80%.

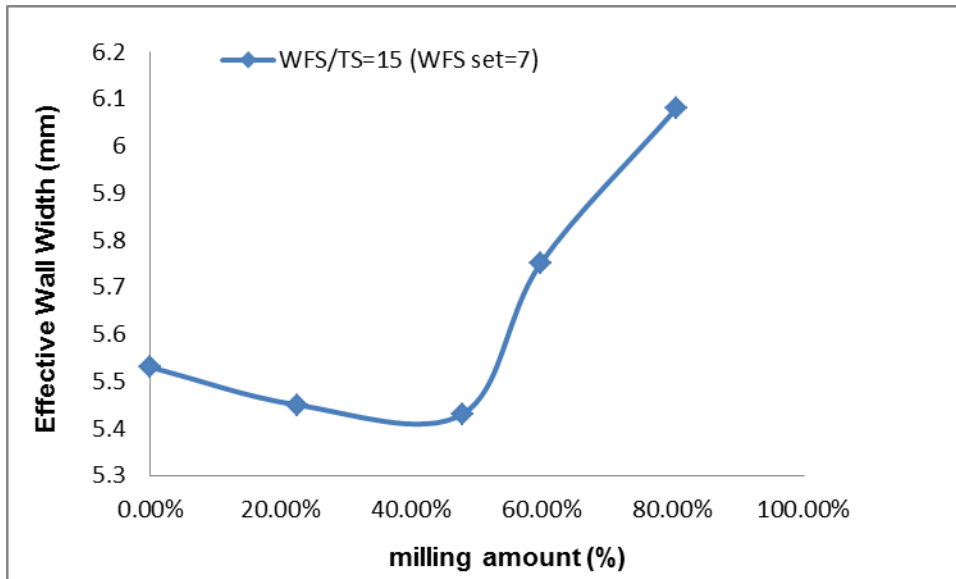


Figure 4-34 Scatter chart about relationship between milling amount and Effective Wall Width (EWW)

4.6.3.2 Effect of milling amount on surface waviness

This section introduces the relationship between SW and milling amount carbon steel walls. According to the scatter chart shown in Figure 4-35 it is observed that surface waviness falls down nearly linear from 0.23 mm to 0.05 mm with milling amount grows up from no milling to 60%, after that, it slightly decreases to 0.04 mm until milling amount is 80%. This figure also gives the true shape of surface waviness, it is easy to find milling amount does not affect surface waviness a lot.

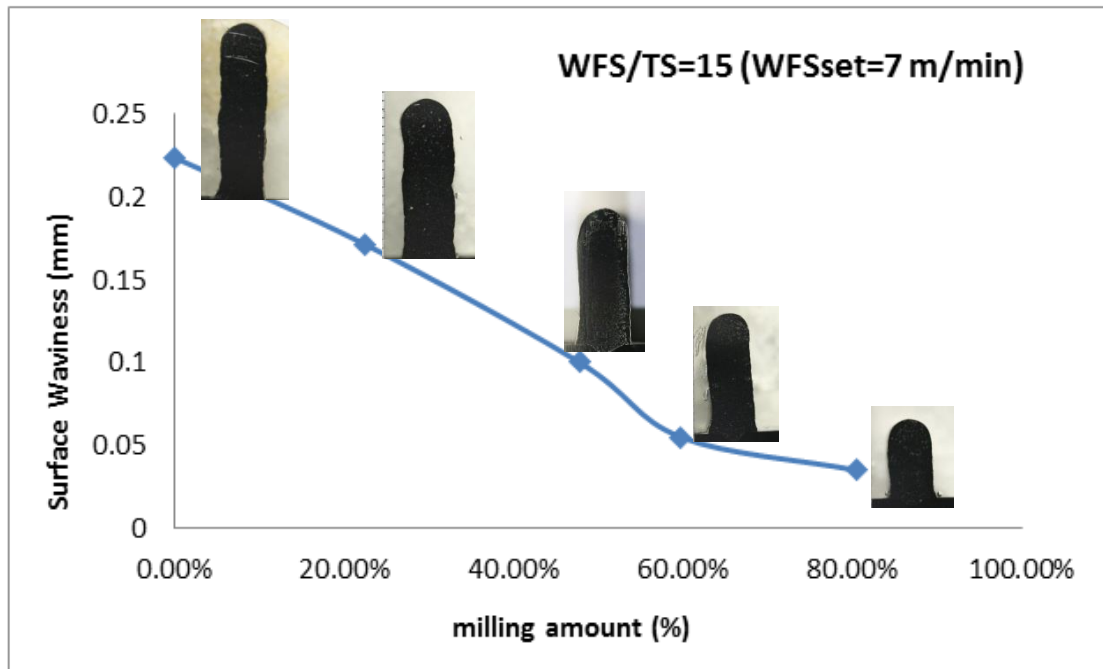


Figure 4-35 Scatter chart about relationship between milling amount and Surface Waviness (compare mild steel S235 with aluminium filler 4043)

4.6.3.3 Effect of milling amount on Material Efficiency

This section reports the results of ME in carbon steel walls for different milling amount. As can be seen in when milling amount is from no milling to 50%, ME declines significantly from 100 % to about 65%, then it shows a fluctuation when milling amount is to 60%, after that, ME keeps drop again from 80% to 55% until milling amount arrives at 80% (see Figure 4-36).

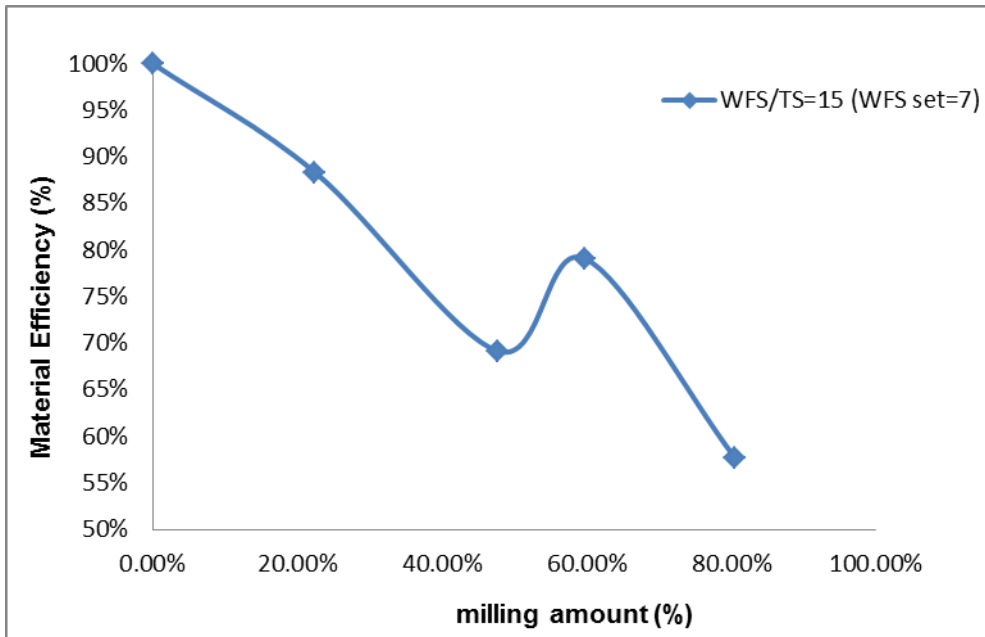


Figure 4-36 Scatter chart about relationship between milling amount and Material Efficiency (compare mild steel S235 with aluminium filler 4043)

4.6.4 Discussion

Friction between the tool and workpiece generates high temperatures, which can cause tool wear and poor surface quality. In order to solve these problems, some strategies have been tried.

A cooling time (about four minutes) was utilised after each layer of deposition. By doing this the temperature before the milling process was controlled. To reduce the temperature that generated by the friction during the milling process, different coolant was investigated. Using liquid coolant during the milling process can reduce the temperature significantly and at the same time it can perform as lubricant between the tool and the workpiece surface. Regardless of the environmental pollution and creates biological problems to the operators of cutting fluids, it aroused another problem. The coolant contaminated the surface which caused serious porosity.

It was reported that the compressed air can be used as a coolant during the milling process. Xiong et al., (2009) did some comparisons for blade abrasions with or without 0.7MPa compressed air cooling and proved that when applying air-blow cooling, the blade abrasion decreases significantly in the same

condition. Finally, 0.7MPa compressed air was used for substitute of liquid coolant through the experiment of milling process on steel, though it could not lubricate the workpiece and tool.

According to the three scatter chart that shown in Figure 4-34, Figure 4-35 and Figure 4-36, comprehensive assess the three factors such as Effective Wall Width, Surface Waviness and Material Efficiency, milling amount arrives at 60% is the optimal choice with the advantages of low Surface Waviness and low waste of materials.

4.7 Summary

Milling amount plays a positive effect on surface waviness and notch radius, plays a negative effect on Material Efficiency when keeping the WFS/TS at a constant ratio.

Bigger notch radius between two layers, smaller surface waviness and rational milling amount make it easy to get small stress concentration factor infinitely near 1 and prolong the fatigue life of the components.

Deposition parameters and milling amount are the potential crucial role that determining the geometry, they affect the shape of the weld bead and covering form of later layer to former layer respectively.

The correlation between SW and milling amount is very similar for both carbon steel (CS) and aluminium (Al) wires (see Figure 4-15 and Figure 4-35).

Integrated deposition and machining process has benefits of controlling geometry and prolonging fatigue life of samples.

5 Experiment on aluminum alloy of deep hole drilling

5.1 Introduction

This chapter discusses the application of the integrated deposition and machining and drilling approach for fabricating deep and small holes. In the dry drilling of Al 4043 alloy, 2 mm diameter short HSS twist drills were used. The integrated deposition and machining processes were the same as described in Chapter 4.

5.2 Experiment

Deep hole drilling experiments were carried out on an aluminium alloy substrate. It is 500 mm long, 100 mm wide and 13 mm thick. Six clamps were used to fix the substrate onto the bed of the HiVE machine. Diamond coated HSS drills with 2 mm in diameter were selected for this project. The length of the drill is 48 mm and effective length is 22 mm. Experiment set-up is shown in Figure 5-1.

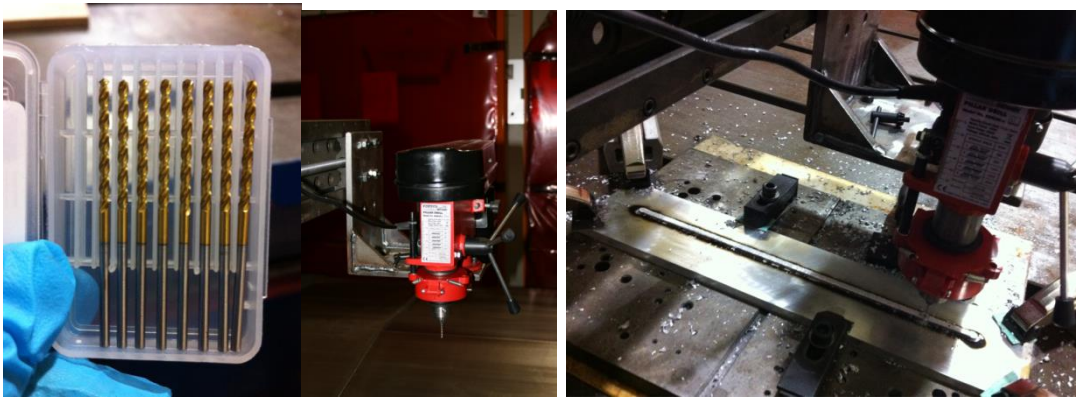


Figure 5-1 Experiment set-up for deep hole drilling

Relevant experiment facilities of small-dimensional deep hole drilling in this research are HiVE machine (see Figure 4-1 a) and manual assembled drilling machine (see Figure 5-1). The manual assembled drilling machine is used to cut holes into or through metal, wood, or other materials. Due to the 2 mm tool diameter chosen in this subject, a spindle with a maximum number of revolutions of 1000 rpm was integrated.

Deposition conditions were the same as which were introduced in Section 4.2.2. The deposition directions were altered for successive layers so that the defects from arc start and arc stop positions on the ends of the wall can be compensated. After the deposition the milling process was used to flat the top surface of the wall and make a constant height increment for each layer of 2 mm. The integrated deposition and milling process was performed for six layers before the drilling process was applied. After that, the same process cycle of deposition milling and drilling was repeated every six layers until the wall reached the required height. Details for procedure of drilling small-dimensional deep holes can be seen in Figure5-2.

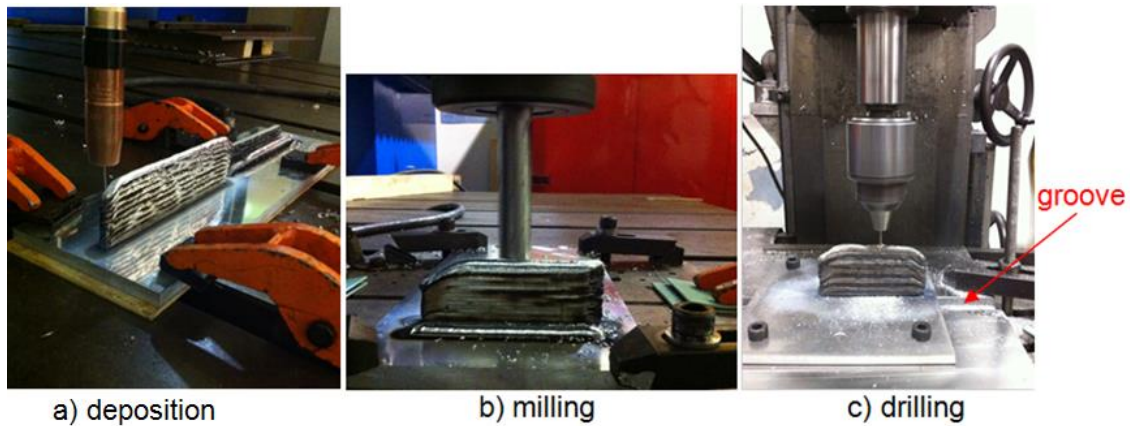


Figure5-2 Procedure of drilling small-dimensional deep holes

A backing plate with a groove was used behind the substrate and aligned with the position of the deposited wall. In the first step the base plate was drilled through to the groove to help the chips from drilling go through. The sample wall was built with 400 mm in length and 126 mm in height. A total of 15 holes with 2 mm in diameter were fabricated evenly along the wall with 25 mm distance between each other.

Through the fundamental experiment, it has been found that milling is a crucial procedure through the whole process for deep hole drilling, otherwise, the drill will slip at the moment it touches the wall because of the circular shape of the weld bead, see Figure 5-3, obviously when this happens it could not guarantee the hole diameter accuracy in rectilinear.



Figure 5-3 Drill slips on the top of weld bead

In the drilling process, the parameters were selected taking into consideration of practical application and requirements in industry. Nouari et al., (2003) finished the experiments of aluminium alloys and obtained the results that cutting speeds ranging from 25 m/min to 165 m/min and with a constant feed rate f of 0.04 mm/rev were all suitable for dry drilling. Considering the capability of the manual assembled drilling machine, spindle speed is automatically controllable (it can be set as fast as 1000 rev/min), but feed rate speed can only be controlled manually. The experiment here was carried out with RPM=850 revs /min, thus, according to the formula below, the cutting speed is 5.338 m/min.

$$RPM(revs/min) = \frac{1000 * \text{cutting speed}(m/min)}{\pi * \text{diameter}(mm)}$$

Where, RPM is the rotational speed of the cutter or workpiece.

Equation 5.1 Formula of calculating cutting speed (Brown and Sharpe, 2013)

The quality of these deep holes was evaluated by X-ray inspection in the last stage. Another small sample was produced to investigate how deep the hole was covered in the subsequent deposition step. In this sample three deep holes were fabricated with the integrated process (as shown in Figure 5-4). The first hole was drilled through. For the second hole the drill process was not used for the last cycle. And for the last hole the drill process was not applied for the last two cycles.

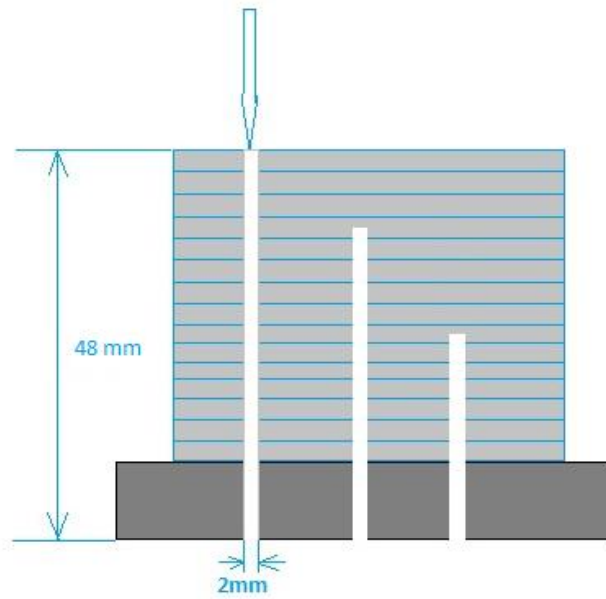


Figure 5-4 Deep hole drilling strategy to see deposition effect on exist small holes

5.3 Results

5.3.1 Straightness of the hole

Figure 5-5 shows the structure which is 400 mm long, 126 mm high wall structure with 15 holes of 2 mm diameter fabricated by integrated deposition and machining (milling and drilling) process according to the methodology introduced in Section 5.2. Figure 5-5 a is the external view of this sample, and Figure 5-5 b) is the photo of X-ray inspection. In general, all 15 holes are through except there is a drill bit inside one of the drilled holes. The straightness of the holes varies a bit mainly because the manual drill was installed onto a platform which was not stiff enough and it vibrated during the drilling process.

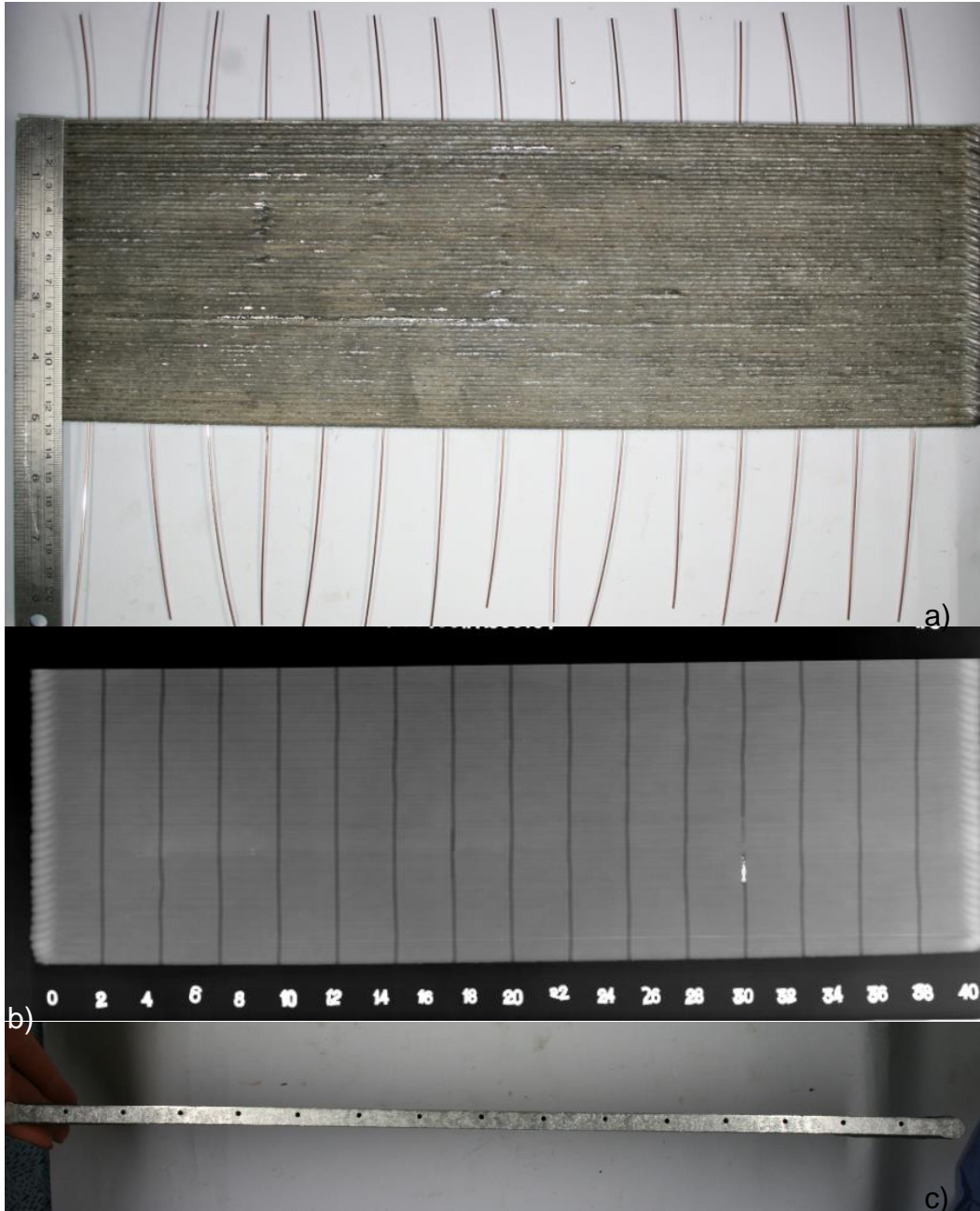


Figure 5-5 Structure manufactured by integrated deposition and machining (milling and drilling) process a) external front view of the structure b) photo of X-ray inspection c) top view of the structure

5.3.2 Depth of material covered on existing holes

Figure 5-6 shows the small 24-layer sample (2 mm each layer) with three holes. The first one is 48 mm deep through-hole for four times drilling. The second one was implemented for three times drilling. The theoretical depth should be 36

mm but the actual depth measured from the X-ray picture was 33.481. So it is obvious that original hole was covered by the subsequent deposition for 2.519 mm. Similarly, the third hole has been applied for two times drilling. The difference between the measured depth and the theoretical depth is 2.764 mm. The depth of the material that covered on the existing holes should be considered in the future to help set up the optimal drilling parameters.

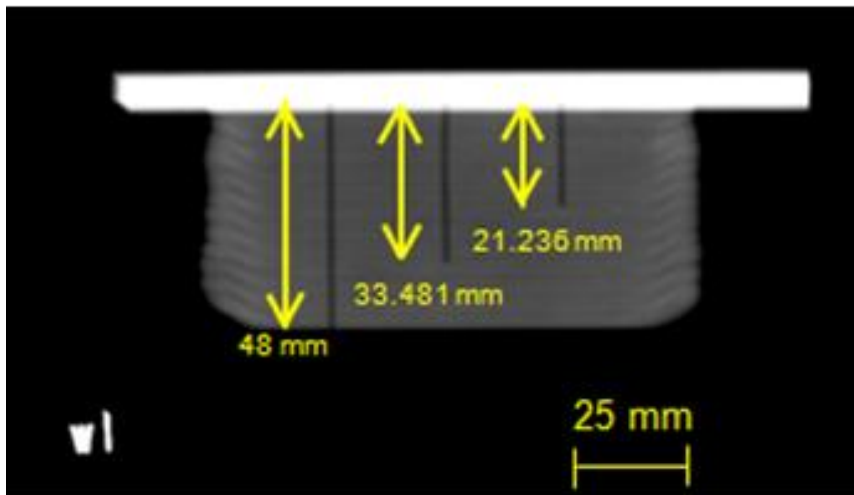


Figure 5-6 Depth measuring through X-ray inspection photo

5.4 Discussion

The discussion here is focused on the features of small-dimension holes of aluminium alloy when using integrated deposition and machining (milling & drilling) process. Here, special attention is given to advantages and limitations of this process for deep hole drilling.

5.4.1 Advantages of this process for deep hole drilling

5.4.1.1 No special requirements for drilling machine and tool

Traditional deep hole drilling requires the use of cutting fluid in drilling process in order to cool and lubricate tool and workpiece, guaranteeing the workpiece quality and making tool life longer. But in fact, none lubrication was used in this process. Some deep hole drilling need special machine and tool, such as Laser microdrilling systems, despite the constant attention, maintenance remained a problem—replacement of the optics, periodic replacement of the flashlamp,

realigning the optics within the laser, and so forth (Rakowski, 2002). However, drilling small-dimensional deep holes using integrated deposition and machining process just need the normal drilling machine and common tool.

5.4.1.2 No limitation on the depth of the holes

Using this integrated deposition with face milling process, no matter how deep the hole is, it is able to make net-shaped metal parts layer by layer with reasonable parameters. This process may also be extended to small channels with angles and curvatures.

5.4.1.3 Meet the accuracy of holes

Figure 5-7 shows the sample fabricated with integrated deposition and drilling, omitting the milling step of each layer. It is clear that the holes are not very straight compared to the sample applying milling step layer by layer, especially the third hole, the hole presents nearly folding line.

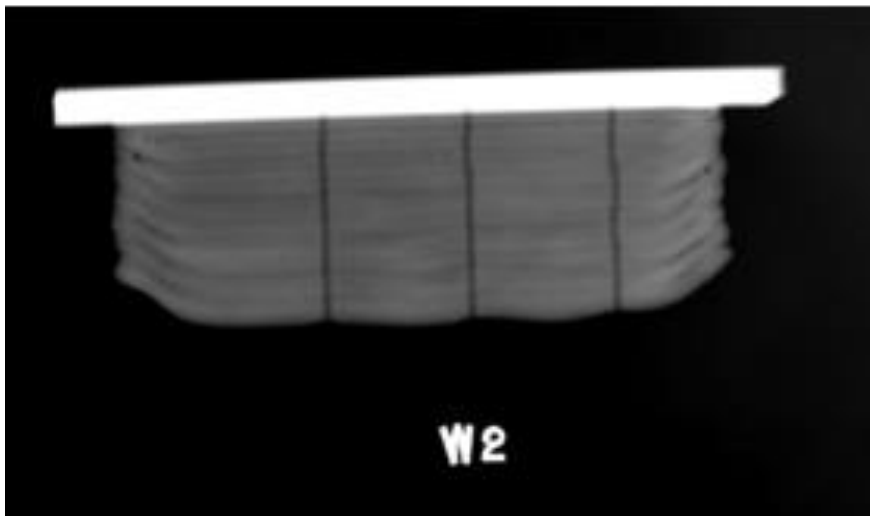


Figure 5-7 X-ray inspection photo of sample without milling

5.4.2 Research limitation

The integrated deposition and machining process for deep hole drilling is only appropriate for small-dimensional deep holes (no more than 3 mm of diameter), the reason is because later deposition will refill the existing hole if the hole is too big enough.

When fabricating thick structure with a good deal of small-dimension holes, it costs a lot of time because feed rate speed could not controlled automatically by this manual assembled drilling machine. In addition, the machine is not very accurate for drilling with significantly shaking of the drill, this is the machine problem itself.

5.5 Summary

This chapter introduces a new strategy of deep hole drilling that difficult or even impossible to finish by traditional drilling method.

The successful fabrication of wall structure with many small-dimensional deep holes demonstrates the potential of the integrated deposition and machining (milling & drilling) process for complex structures with small-dimensional deep holes.

6 General Conclusions

This thesis has investigated integrated deposition and machining of Al using WAAM process, finding relationship between milling amount, surface waviness and fatigue life, which is a necessary process for fabricating the structures with some special position impossible to be machined or hard materials difficult for machining.

The following conclusions can be drawn from the present study:

- The CMT plus Pulse Advanced (CMT-PADV) process is appropriate for Wire and Arc Additive Manufacturing of aluminum applications because of its excellent deposition characteristics, high deposition rate, arc welding stability and low heat input.
- The surface finishing of the WAAM wall can be significantly improved by using the integrated deposition and milling process.
- Two major factors affect surface waviness and radius, the first one is deposition parameters, which decides the shape of the weld bead, and another one is milling amount, which gives significant effect on overlap form.
- When milling amount increase, mild steel S235 has similar trend to aluminum 4043 filler on behavior of surface waviness, effective wall width and material efficiency.
- The integrated deposition and milling process can produce walls with smaller surface waviness and larger notch radius which result in smaller stress concentration factors.
- The successful fabrication of high metallic parts with many small-dimensional deep holes demonstrates the potential of the integrated deposition and machining (milling & drilling) process for complex structures with small-dimensional deep holes.

7 Future Work

According to the research contents and the expected development of WAAM process, many other researches can be performed on the following aspects:

- It is well known that how to control porosity is always a challenge for fabricating aluminium structures using weld-related process such as WAAM. Fatigue life of samples can be dramatically reduced by any pore inside or close to the surface. Thus, fatigue test (tensile and compressive stress) and other mechanical testing should be done after solving the problem of porosity to verify whether the structures are in acceptable fatigue life that can be used directly without end machining and where is the stress concentration of the samples and whether radius is the main influencing factor.
- Fabricating three large scale structures with three kinds of manufacturing process, one for traditional manufacturing and the others for identical deposition and milling using WAAM (one for WAAM & end milling, another for integrated deposition and machining process), examining how this process is competitive compared with the conventional milling operation and normal WAAM with end milling in terms of manufacturing time and the Buy-to-Fly ratio.
- Compare the normal deposition of aluminium with integrated deposition and machining process, microstructure study and analysis on ductility and fracture should be investigated. In addition, research should be done to see whether using integrated deposition and machining process is an effective way for solving the problem of porosity of aluminium alloy.
- Integrated deposition and machining (milling & drilling) process should be applied to fabricate more complex structures with curving channel. Furthermore, experimental analysis should be aim at tool wear of dry drilling preventing drill broken in exist holes.

REFERENCES

- Adebayo, A., Mehnen, J. and Tonnelier, X. (2013), "Effects of solid lubricants on wire and arc additive manufactured structures", *Proceedings of the Institution of Mechanical Engineers, Part B: Journal of Engineering Manufacture*, vol. 1, no. SAGE, pp. 8.
- Adler, D., Hii, W., Michalek, D. and Sutherland, J. (2006), "Examining the role of cutting fluids in machining and efforts to address associated environmental/health concerns", *Machining Science and Technology*, vol. 10, no. 1, pp. 23-58.
- Akula, S. and Karunakaran, K. (2006), "Hybrid adaptive layer manufacturing: An Intelligent art of direct metal rapid tooling process", *Robotics and Computer-Integrated Manufacturing*, vol. 22, no. 2, pp. 113-123.
- Alam, M. M. (2012), *Laser welding and cladding: The effects of defects on fatigue behaviour* (PhD thesis), Luleå University of Technology, Sweden.
- Almeida, P. S. and Williams, S. (2010), "Innovative process model of Ti-6Al-4V additive layer manufacturing using cold metal transfer (CMT)", *Proceedings of the Twenty-first Annual International Solid Freeform Fabrication Symposium, University of Texas at Austin, Austin, TX, USA*, .
- Baufeld, B., Biest, O. V. d. and Gault, R. (2010), "Additive manufacturing of Ti-6Al-4V components by shaped metal deposition: Microstructure and mechanical properties", *Materials & Design*, vol. 31, pp. S106-S111.
- Biermann, D., Heilmann, M. and Kirschner, M. (2011), "Analysis of the influence of tool geometry on surface integrity in single-lip deep hole drilling with small diameters", *Procedia Engineering*, vol. 19, pp. 16-21.
- Brown and Sharpe (2013), *Speeds and feeds*, available at: http://en.wikipedia.org/wiki/Speeds_and_feeds (accessed October).
- Canter, N. (2009), "The possibilities and limitations of dry machining", *Tribology & lubrication technology*, vol. 65, no. 3, pp. 40-44.
- Chapetti, M. and Jaureguizar, L. (2011), "Estimating the fatigue behaviour of welded joints", *Procedia Engineering*, vol. 10, pp. 959-964.
- Chen, J. (2012), *Hybrid design based on wire and arc additive manufacturing in the aircraft industry* (MSc thesis), Cranfield University, Cranfield, UK.
- Chern, T., Tseng, K. and Tsai, H. (2011), "Study of the characteristics of duplex stainless steel activated tungsten inert gas welds", *Materials & Design*, vol. 32, no. 1, pp. 255-263.
- CHIRON (2012), *Ahead through experience*, available at: <http://www.chiron.de/en/home/industry-solutions/industry-overview/aerospace.html> (accessed November).
- Cozzolino. (Cranfield University), (2013), *Shielding gas optimisation study for wire arc additive manufacture* (unpublished Technical Report), Welding Engineering And Laser Processing Centre.

- Da Silva, Celina Leal Mendes and Scotti, A. (2006), "The influence of double pulse on porosity formation in aluminum GMAW", *Journal of Materials Processing Technology*, vol. 171, no. 3, pp. 366-372.
- Ding, J. (2012), "*Thermo-mechanical analysis of wire and arc additive manufacturing process*" (PhD thesis), Cranfield University, Cranfield, UK.
- Ding, J., Colegrove, P., Mehnen, J., Ganguly, S., Sequeira Almeida, P., Wang, F. and Williams, S. (2011), "Thermo-mechanical analysis of Wire and Arc Additive Layer Manufacturing process on large multi-layer parts", *Computational Materials Science*, vol. 50, no. 12, pp. 3315-3322.
- Donlon, W., Paige, C., Morris, C. and Allison, J. (1996), "The effects of casting defects and microstructure on the mechanical properties of die cast AM 50 magnesium and 356 aluminum", *Minerals, Metals and Materials Society/AIME(USA)*, vol. 1, no. 1, pp. 17-27.
- Fessler, J., Merz, R., Nickel, A., Prinz, F. B. and Weiss, L. (1996), "Laser deposition of metals for shape deposition manufacturing", *Proceedings of the Solid Freeform Fabrication Symposium*, University of Texas at Austin, pp. 117.
- Fronius (2010), *CMT Advanced*, available at: http://www.axson.se/res/broschyre/pdf/fro_bro_cmt_advanced_eng.pdf (accessed May).
- Gibson, I., Rosen, D. W. and Stucker, B. (2010), *Additive manufacturing technologies: rapid prototyping to direct digital manufacturing*, Springer.
- Heikki Tikkinen (2010), *Deep hole drilling*, available at: http://webhotel2.tut.fi/projects/caeds/tekstit/machining/machining_drilling.pdf (accessed August).
- Jeng, J. and Lin, M. (2001), "Mold fabrication and modification using hybrid processes of selective laser cladding and milling", *Journal of Materials Processing Technology*, vol. 110, no. 1, pp. 98-103.
- Junyan, L., Huanpeng, L., Rongdi, H. and Yang, W. (2010), "The study on lubrication action with water vapor as coolant and lubricant in cutting ANSI 304 stainless steel", *International Journal of Machine Tools and Manufacture*, vol. 50, no. 3, pp. 260-269.
- Kai, C. C., Fai, L. K. and Chu-Sing, L. (eds.) (2003), *Rapid prototyping: principles and applications in manufacturing*, 3rd ed, World Scientific Publishing Co., Inc., River Edge, NJ, USA.
- Karunakaran, K., Suryakumar, S., Pushpa, V. and Akula, S. (2010), "Low cost integration of additive and subtractive processes for hybrid layered manufacturing", *Robotics and Computer-Integrated Manufacturing*, vol. 26, no. 5, pp. 490-499.
- Kazanas, P., Deherkar, P., Almeida, P., Lockett, H. and Williams, S. (2012), "Fabrication of geometrical features using wire and arc additive manufacture", *Proceedings of the Institution of Mechanical Engineers, Part B: Journal of Engineering Manufacture*, vol. 226, no. 6, pp. 1042-1051.

- Kurt, M., Bagci, E. and Kaynak, Y. (2009), "Application of Taguchi methods in the optimization of cutting parameters for surface finish and hole diameter accuracy in dry drilling processes", *The International Journal of Advanced Manufacturing Technology*, vol. 40, no. 5-6, pp. 458-469.
- Lahres, M., Müller-Hummel, P. and Doerfel, O. (1997), "Applicability of different hard coatings in dry milling aluminium alloys", *Surface and Coatings Technology*, vol. 91, no. 1, pp. 116-121.
- Lassen, T. (1990), "The effect of the welding process on the fatigue crack growth", *Welding Journal*, vol. 69, pp. 75S-81S.
- Legait, P. (2006), *Formation and distribution of porosity in Al-Si welds* (MSc thesis), Worcester Polytechnic Institute, USA.
- Martina, F., Mehnen, J., Williams, S., Colegrove, P. and Wang, F. (2012), "Investigation of the benefits of plasma deposition for the additive layer manufacture of Ti-6Al-4V", *Journal of Materials Processing Technology*, vol. 212, no. 6, pp. 1377-1386.
- Mayer, H., Lipowsky, H., Papakyriacou, M., Rosch, R., Stich, A., Zetti, B. and Stanzl-Tschegg, S. (1999), "Fatigue properties of high pressure die cast magnesium alloys at high numbers of cycles", *Fatigue'99: Seventh International Fatigue Congress*, pp. 2059.
- Mehnen, J., Ding, J., Lockett, H. and Kazanas, P. (2011), "Design for wire and arc additive layer manufacture", in *Global Product Development*, Springer, , pp. 721-727.
- Mok, S. H., Bi, G., Folkes, J. and Pashby, I. (2008), "Deposition of Ti-6Al-4V using a high power diode laser and wire, Part I: Investigation on the process characteristics", *Surface and Coatings Technology*, vol. 202, no. 16, pp. 3933-3939.
- Nouari, M., List, G., Girot, F. and Coupard, D. (2003), "Experimental analysis and optimisation of tool wear in dry machining of aluminium alloys", *Wear*, vol. 255, no. 7, pp. 1359-1368.
- Pickin, C. and Young, K. (2006), "Evaluation of cold metal transfer (CMT) process for welding aluminium alloy", *Science and Technology of Welding & Joining*, vol. 11, no. 5, pp. 583-585.
- Praveen, P. and Yarlagadda, P. (2005), "Meeting challenges in welding of aluminum alloys through pulse gas metal arc welding", *Journal of Materials Processing Technology*, vol. 164, pp. 1106-1112.
- Rakowski, L. (2002), "Non-traditional methods for making small holes", *Modern Machine Shop(USA)*, vol. 75, no. 1, pp. 76-83.
- Rendigs, K. and Knowler, M. (2010), "Metal materials in Airbus A380", *2nd Izmir Global Aerospace & Offset Conference, Izmir, Turkey*, .
- Richard, S. (1995), *The procedure handbook of arc welding*, 1st ed, The Lincoln Electric Company, Cleveland, Ohio.

- Richardson, R. and Bhatti, R. (2001), "A review of research into the role of guide pads in BTA deep-hole machining", *Journal of Materials Processing Technology*, vol. 110, no. 1, pp. 61-69.
- Rosen, D. W. (2007), "Computer-aided design for additive manufacturing of cellular structures", *Computer-Aided Design & Applications*, vol. 4, no. 5, pp. 585-594.
- Rösler, J., Harders, H. and Bäker, M. (2007), *Mechanical behaviour of engineering materials: metals, ceramics, polymers, and composites*, Springer.
- Santos, E. C., Shiomi, M., Osakada, K. and Laoui, T. (2006), "Rapid manufacturing of metal components by laser forming", *International Journal of Machine Tools and Manufacture*, vol. 46, no. 12, pp. 1459-1468.
- Sequeira Almeida, P. M. (2012), "Process control and development in wire and arc additive manufacturing" (PhD thesis), Cranfield University, Cranfield, UK.
- SMU (2012), *Research Center for Advanced Manufacturing*, available at: <http://www.smu.edu/Lyle/Departments/ME/Research/RCAM> (accessed July).
- Song, Y., Park, S., Hwang, K., Choi, D. and Jee, H. (1998), "3D welding and milling for direct prototyping of metallic parts", *Proceedings of the Solid Freeform Fabrication Symposium, University of Texas at Austin*, pp. 495.
- Song, Y., Park, S., Choi, D. and Jee, H. (2005), "3D welding and milling: Part I – a direct approach for freeform fabrication of metallic prototypes", *International Journal of Machine Tools and Manufacture*, vol. 45, no. 9, pp. 1057-1062.
- Spencer, J., Dickens, P. and Wykes, C. (1998), "Rapid prototyping of metal parts by three-dimensional welding", *Proceedings of the Institution of Mechanical Engineers, Part B: Journal of Engineering Manufacture*, vol. 212, no. 3, pp. 175-182.
- Sreejith, P. and Ngoi, B. (2000), "Dry machining: machining of the future", *Journal of Materials Processing Technology*, vol. 101, no. 1, pp. 287-291.
- Sun, S., Brandt, M. and Dargusch, M. (2010), "Machining Ti–6Al–4V alloy with cryogenic compressed air cooling", *International Journal of Machine Tools and Manufacture*, vol. 50, no. 11, pp. 933-942.
- Taminger, K. M. and Hafley, R. A. (2002), "Characterization of 2219 aluminum produced by electron beam freeform fabrication", *Proceedings of 13th SFF symposium*, pp. 482.
- Tönshoff, H., Spintig, W., König, W. and Neises, A. (1994), "Machining of holes developments in drilling technology", *CIRP Annals-Manufacturing Technology*, vol. 43, no. 2, pp. 551-561.
- Wang, F., Williams, S., Colegrove, P. and Antonysamy, A. A. (2013), "Microstructure and Mechanical Properties of Wire and Arc Additive

- Manufactured Ti-6Al-4V", *Metallurgical and Materials Transactions A*, vol. 44, no. 2, pp. 968-977.
- Wang, H., Jiang, W., Ouyang, J. and Kovacevic, R. (2004), "Rapid prototyping of 4043 Al-alloy parts by VP-GTAW", *Journal of Materials Processing Technology*, vol. 148, no. 1, pp. 93-102.
- Webster, G. and Ezeilo, A. (2001), "Residual stress distributions and their influence on fatigue lifetimes", *International Journal of Fatigue*, vol. 23, pp. 375-383.
- Xavier, L. F. and Elangovan, D. (2013), "Effective Parameters For Improving Deep Hole Drilling Process By Conventional Method-A Review", *International Journal of Engineering*, vol. 2, no. 3, pp. 1.
- Xiong, X., Zhang, H. and Wang, G. (2009), "Metal direct prototyping by using hybrid plasma deposition and milling", *Journal of Materials Processing Technology*, vol. 209, no. 1, pp. 124-130.
- Yue, Y., Gunter, K. L., Michalek, D. J. and Sutherland, J. W. (1999), "An examination of cutting fluid mist formation in turning", *TRANSACTIONS-NORTH AMERICAN MANUFACTURING RESEARCH INSTITUTION OF SME*, , pp. 221-226.
- Zabel, A. and Heilmann, M. (2012), "Deep hole drilling using tools with small diameters—Process analysis and process design", *CIRP Annals-Manufacturing Technology*, vol. 61, no. 1, pp. 111-114.
- Zhai, Y. (2012), "*Early cost estimation for additive manufacture*" (MSc thesis), Cranfield University, Cranfield, UK.

APPENDICES

Appendix A Measurement of samples

Table A- 1 Detail data of samples with WFS at 7.5 m/min in al

Sample	Milling amount (%)	Effective Wall Width (mm)	Surface waviness (mm)	ME (%)	Radius (mm)	SCF
A	0	5.78	0.298	100	0.178	3.453
A1	26.25	6.12	0.167	96.31	0.205	2.223
A2	40.48	6.47	0.158	56.67	0.508	1.676
A3	54.95	6.79	0.146	45.53	0.7	1.45
A4	71.43	7.31	0.075	36.67	0.9	1.266

Table A- 2 Detail data of samples with WFS at 6.5 m/min in al

Sample	Milling amount (%)	Effective Wall Width (mm)	Surface waviness (mm)	ME (%)	Radius (mm)	SCF
B	0	6.06	0.325	100	0.263	3.089
B1	19.70	6.39	0.236	88.76	0.222	2.457
B2	37.89	6.66	0.215	77.42	0.241	2.337
B3	52.33	6.92	0.124	65.54	0.607	1.592
B4	69.04	7.23	0.060	49.95	1.098	1.344

Table A- 3 Detail data of samples with WFS at 5.5 m/min in al

Sample	Milling amount (%)	Effective Wall Width (mm)	Surface waviness (mm)	ME (%)	Radius (mm)	SCF
C	0.00%	6.37	0.334	100	0.355	3.462
C2	30.23%	6.2	0.249	80.84	0.562	2.739
C3	47.06%	6.73	0.143	66.04	0.989	1.759
C4	64.83%	6.95	0.071	44.90	1.809	1.324

Table A- 4 Detail data of samples with WFS at 4.5 m/min in al

Sample	Milling amount (%)	Effective Wall Width (mm)	Surface waviness (mm)	ME (%)	Radius (mm)	SCF
D	0.00%	6.22	0.299	100	0.306	2.65
D2	25.19%	6.53	0.211	83.60	0.463	1.895
D3	43.96%	6.74	0.094	66.46	0.756	1.465
D4	61.49%	6.96	0.083	51.63	2.337	1.198

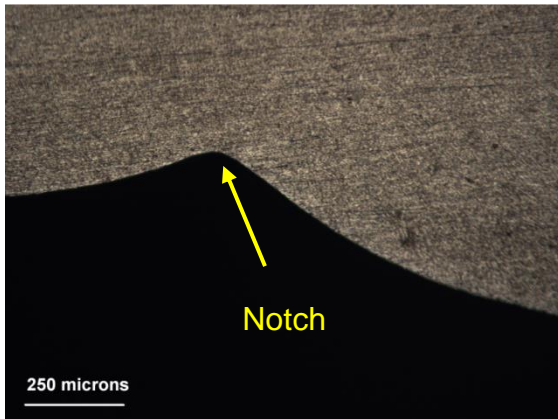
Table A- 5 Detail data of samples with WFS at 3.5 m/min in al

Sample	Milling amount (%)	Effective Wall Width (mm)	Surface waviness (mm)	ME (%)	Radius (mm)	SCF
E	0.00%	5.84	0.372	100.0	0.041	3.599
E2	22.98%	5.84	0.237	72.63	0.058	2.936
E3	42.46%	6.24	0.070	63.65	0.625	2.487
E4	59.57%	6.42	0.080	48.01	1.434	1.398

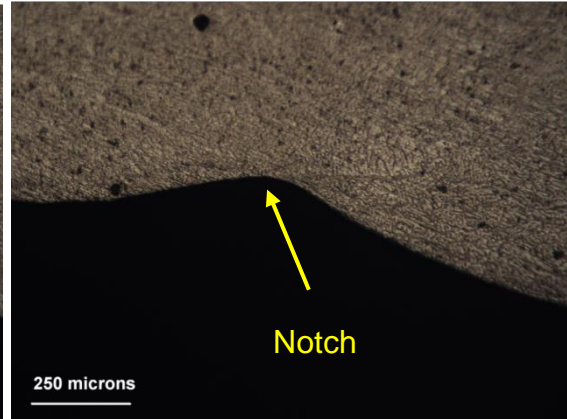
Table A- 6 Detail data of samples with WFS at 7.0 m/min in mild steel

Sample	Milling amount (%)	Effective Wall Width (mm)	Surface waviness (mm)	ME (%)
J	0.00%	5.53	0.223	100
J1	22.41%	5.45	0.171	88.35
J2	47.71%	5.43	0.1	69.17
J3	59.68%	5.75	0.055	79.11
J4	80.46%	6.08	0.035	57.71

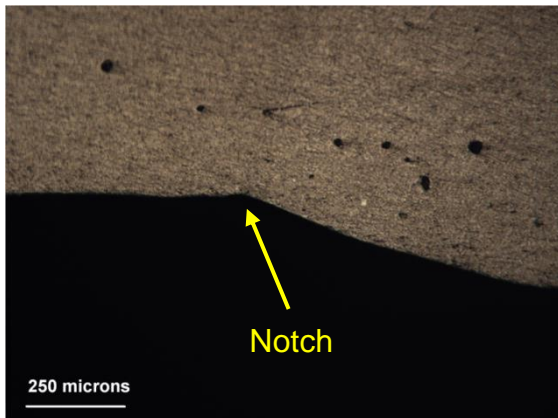
Appendix B Obvious changes of notch in aluminium



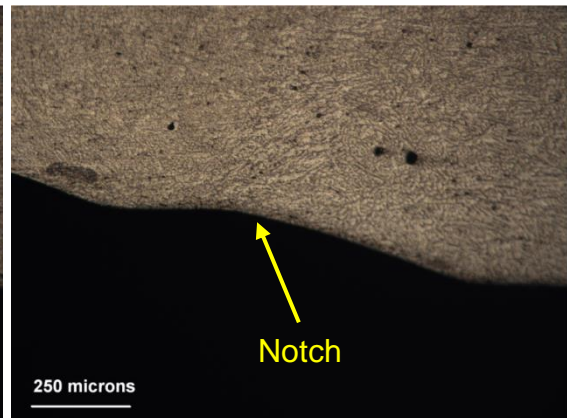
Milling amount: 25%



Milling amount: 40%



Milling amount: 55%



Milling amount: 70%

Figure B- 1 The obvious changes of notch from sharp to flat with different milling amount increases from 25% to 70%

Appendix C Problems that happened during the experiment



Figure C- 1 Walls got poor quality when there was no shielding gas during the deposition process



Figure C- 2 Too small WFS (first layer) resulted in low current and small dilution, layer separated from substrate after milling was done

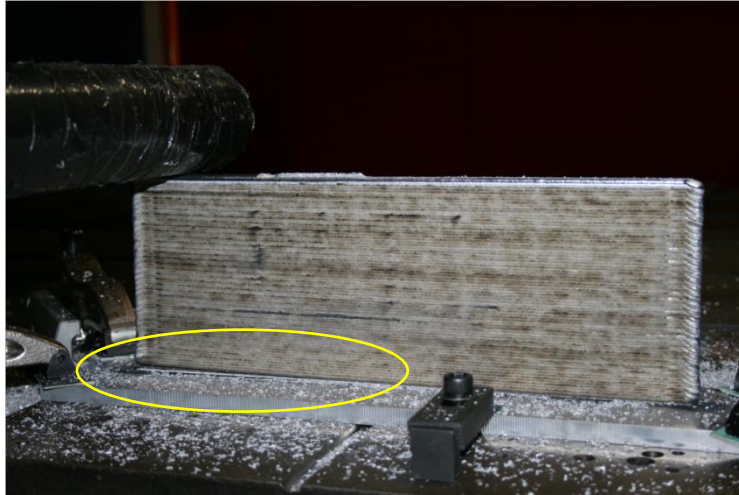


Figure C- 3 Joint flaws between wall and substrate, WFS set should be increased for the first layer



Figure C- 4 Holes present nearly folding line because of drill slipping the top of weld bead



Figure C- 5 Wrong setting of operating program resulted in the broken of workpiece and machining tool